

For submission to MNRAS. Not for distribution

## **The Formation and Evolution of Virgo Cluster Galaxies – II. Stellar Populations**

Joel C. Roediger and Stéphane Courteau

*Department of Physics, Engineering Physics & Astronomy, Queen's University, Kingston,  
Ontario, Canada*

Lauren A. MacArthur

*Herzberg Institute of Astrophysics, National Research Council of Canada, 5071 West Saanich  
Road, Victoria, BC, Canada*

and

Michael McDonald

*Dept. of Astronomy, University of Maryland, College Park, MD*

jroediger, courteau@astro.queensu.ca, Lauren.MacArthur@nrc-cnrc.gc.ca,  
mcdonald@astro.umd.edu

### **ABSTRACT**

We use a combination of deep optical and near-infrared light profiles for a morphologically diverse sample of Virgo cluster galaxies to study the radially-resolved stellar populations of cluster galaxies over a wide range of galaxy structure. We find that, in the median, the age gradients of Virgo galaxies are either flat (lenticulars and Sa–Sb spirals) or positive (ellipticals, Sbc+Sc spirals, gas-rich dwarfs, and irregulars), while all galaxy types have a negative median metallicity gradient. Comparison of the galaxy stellar population diagnostics (age, metallicity, and gradients thereof) against structural and environmental parameters also reveals that the ages of gas-rich systems depend mainly on their atomic gas deficiencies. Conversely, the metallicities of Virgo gas-poor galaxies depend on their concentrations, luminosities, and surface brightnesses. The stellar population gradients of all Virgo galaxies exhibit no dependence on either their structure or environment. The stellar populations of gas-poor giants

(E/S0) are consistent with a hierarchical formation, wherein the stars in more massive systems were largely formed out of dissipative starbursts associated with gas-rich merging. Differences in the stellar population properties of gas-poor dwarfs and giants suggests different origins for them. The stellar populations in Virgo dS0's and dE's also lack uniformity, suggesting that the formation of Virgo gas-poor dwarfs proceeded through at least two different channels (environmental transformation and merging). Lastly, the present stellar content of Virgo spirals seems to have been largely regulated by environmental effects. Spirals with positive age gradients (largely gas-poor types) are likely evolutionary remnants of progenitors which were stripped of their gas disks due to prolonged exposure to the intercluster medium wind. Spirals with negative age gradients are consistent with a traditional inside-out disk growth scenario and have likely not been affected by their environment yet. The paucity of flat stellar population gradients in Virgo spirals suggests that secular evolution is likely not responsible for the formation of their bulges.

*Subject headings:* galaxies: clusters: individual (Virgo) — galaxies: dwarf — galaxies: elliptical — galaxies: lenticular — galaxies: evolution — galaxies: formation — galaxies: irregular — galaxies: peculiar — galaxies: spiral — galaxies: stellar content — galaxies: structure

## 1. INTRODUCTION

While successes of the  $\Lambda$ CDM cosmological model (Springel et al. 2005) suggest that galaxies formed through the merging of smaller units, this model still cannot explain many basic galaxy observables (e.g., Klypin et al. 1999; Noeske et al. 2007; Dutton 2009), all of which underscore the importance of the thermal and dynamical interplay between baryons, feedback, and dark matter during galaxy formation (Baugh 2006). Since this interplay involves the processes of star formation (SF) and interstellar medium (ISM) enrichment, study of galaxies' stellar populations yields fundamental constraints for galaxy formation models. With this in mind, we present a homogeneous analysis of the stellar populations of Virgo cluster galaxies, based on an extensive multi-band photometric database (McDonald et al. 2011, Roediger et al. 2011, hereafter Paper I). The use of a cluster sample is advantageous as it encompasses all galaxy types within a relatively small angular area and at a common distance. To further motivate our work, we highlight below the specific unknowns regarding the formation and evolution of basic galaxy types (gas-poor giants and dwarfs, and spirals), and how stellar population data may help. The initiated reader may skip to §1.4.

## 1.1. Giant gas-poor galaxies

Since the first simulations of binary disk mergers showed that such events produce remnants with spheroidal morphologies (Toomre & Toomre 1972), giant gas-poor galaxies (E/S0's) have come to be regarded as the prototypical byproduct of hierarchical merging in  $\Lambda$ CDM cosmology. Supporting evidence for the hierarchical origin of E/S0's now includes the time evolution of the galaxy merger rate (e.g., Conselice et al. 2003b), the existence of (ultra-)luminous infrared and sub-millimeter galaxies (Sanders & Mirabel 1996; Smail et al. 1997), and the photometric, structural, and kinematical properties of local gas-poor giants on both local and global scales (e.g., Faber et al. 1997; van Dokkum 2005; Côté et al. 2006; Emsellem et al. 2007). Whether the mergers which may have created E/S0's were gas-rich, gas-poor, or some combination thereof remains unknown, but high-redshift observations of galaxy mergers and sizes, as well as input from simulations, suggest that some amount of gas-poor merging is vital to the growth, shapes, and kinematics of massive E/S0's (Bell et al. 2006; Naab et al. 2006; van der Wel et al. 2008).

Despite much support for a hierarchical origin of giant gas-poor galaxies, the discovery that stellar ages and  $\alpha$ -enhancements in local E/S0's decrease to low masses (i.e., “downsizing”; Caldwell et al. 2003; Nelan et al. 2005; Thomas et al. 2005; Clemens et al. 2006; Smith et al. 2007) has been difficult to reconcile within this scenario (but see Bower et al. 2006, De Lucia et al. 2006 and Neistein et al. 2006). This stems from the fact that downsizing implies that more massive E/S0's formed their stars earlier and faster than less massive ones, trends which more readily agree with a monolithic collapse scenario (Eggen et al. 1962; Larson 1974). The downsizing phenomenon has thus created an impetus to measure other stellar population diagnostics for gas-poor giants, such as metallicity gradients<sup>1</sup> (Foster et al. 2009, and references therein), to compare with merger (Hopkins et al. 2009b) and collapse (Pipino et al. 2008) simulations.

In monolithic collapse, a giant gas cloud undergoes a galaxy-wide starburst as it rapidly collapses to its center, leaving remnants with shallow, positive age gradients, while their metallicity gradients would be steep and negative due to the cumulative enrichment of their central regions by SNe (Kobayashi 2004; Pipino et al. 2008). On the other hand, the stellar population gradients of merger remnants should span a large range, determined primarily by the progenitors' gas fractions. That is, the central starburst in a gas-rich merger (Hernquist & Mihos 1995) will create a positive age and negative metallicity gradient within the remnant's innermost kiloparsec (Hopkins et al. 2009b), while violent relaxation will tend to flatten the stellar population gradients within a gas-poor merger remnant (White 1980; Hopkins et al. 2009c), unless the progenitors' gradients are steep (Di Matteo et al. 2009). Comparisons of the above predictions with stellar population gradients measured in E/S0's has however led to conflicting results (Tamura & Ohta

---

<sup>1</sup>By “gradient,” we refer to the radial behaviour of a given quantity in a galaxy.

2003; Michard 2005; Wu et al. 2005; Foster et al. 2009; Koleva et al. 2009; Spolaor et al. 2009; Tortora et al. 2010). Given the difficulty of obtaining deep, high signal-to-noise spectra for such galaxies, statistical studies of this sort, based on a photometric approach, are highly desirable (e.g., La Barbera et al. 2010).

## 1.2. Dwarf gas-poor galaxies

The formation scenarios for giant gas-poor galaxies would also be relevant to their dwarf counterparts (dE/dS0) if the latter simply represented the extension of the former to low luminosities. Although the near-orthogonal structural scaling relations of gas-poor dwarfs and giants have been used as evidence against their common origin (e.g., Kormendy et al. 2009; but see Ferrarese et al. 2006a and references therein), Graham & Guzmán (2003) have shown that all gas-poor galaxies populate a continuous manifold when these relations are expanded to include the Sérsic  $n$  index. This manifold also explains why light profiles vary between gas-poor dwarfs ( $n \sim 1$ ) and giants ( $n \sim 4$ ). Moreover, all gas-poor galaxies follow a single scaling relation between the mass of their central compact objects (supermassive black holes or nuclear star clusters) and the velocity dispersion of the galaxy spheroids (Ferrarese et al. 2006b). From the cosmological perspective, a hierarchical formation of dwarf gas-poor galaxies appears plausible as  $\Lambda$ CDM merger trees may truncate at low masses (Valcke et al. 2008). A summary of additional evidences that favour a common origin for all gas-poor galaxies is presented in Graham & Guzmán (2003).

Alternatively, gas-poor dwarfs may represent the evolutionary remnants of gas-rich dwarfs which had their gas supply removed. This scenario is supported by several evidences: (i) both dwarf galaxy types exhibit exponential light profiles (Lin & Faber 1983), (ii) unsharp masking of cluster gas-poor dwarf galaxy images reveals a high frequency of weak stellar disks, spiral arms and bars (Jerjen et al. 2000; Barazza et al. 2002; Graham et al. 2003; Lisker et al. 2006a), (iii) the size-luminosity trends exhibited by dwarf and giant gas-poor Virgo cluster galaxies disagree (Janz & Lisker 2008), (iv) many cluster dE’s possess significant rotational support (Pedraz et al. 2002, De Rijcke et al. 2003, van Zee et al. 2004a; but see Geha et al. 2002), (v) unlike Virgo E/S0’s, dE’s (van Zee et al. 2004b) had extended star formation histories as gauged by their low stellar  $\alpha$ -enhancements, (vi) some Virgo dE’s possess gas disks (Conselice et al. 2003a; De Rijcke et al. 2003; Lisker et al. 2006b), and (vii) gas-poor dwarfs are mainly found in high-density environments, as opposed to gas-poor giants (e.g., Haines et al. 2006).

An evolutionary origin of gas-poor dwarfs would likely be the result of an external (environmental) trigger. Supporting evidence of such a trigger includes the segregation of gas-poor dwarfs to the centers of galaxy groups and clusters (Binggeli et al. 1990) and the susceptibility of both the structure and gas content of dwarf galaxies to external influences (Mayer et al. 2001,

2006). Internal triggers of such an evolution, like gas exhaustion and/or expulsion, may only play secondary roles as suggested by simulations (Mac Low & Ferrara 1999), simple physical arguments (Grebel et al. 2003) and the extended star formation histories of Local Group dwarf galaxies (Tolstoy et al. 2009). Environmental triggers come in one of two broad flavours, tidal (Moore et al. 1996) and hydrodynamic (Gunn & Gott 1972), but the observed stripping of (more massive) cluster spirals (Chung et al. 2009) and the correlation of cluster gas-rich dwarfs’  $H\alpha$  emission with their gas deficiency but not their cluster-centric location (Gavazzi et al. 2006), both suggest that gas-rich dwarfs would more likely be victims of the latter. Indeed, Boselli et al. (2008,b) have demonstrated that ram-pressure stripping and subsequent fading of gas-rich dwarfs explain the integrated, multi-wavelength SEDs and structural scaling relations of Virgo dE/dS0’s. A study of some of these galaxies’ stellar populations (van Zee et al. 2004b) yielded a similar conclusion.

Despite the compelling similarities between gas-rich and gas-poor dwarfs, Lisker et al. (2006a,b, 2007, 2009), Toloba et al. (2009), Kim et al. (2010), and Paudel et al. (2010) have shown that morphological subgroups (i.e., “normal”, disk, blue center, etc.) exist amongst Virgo dE’s and that this diversity correlates with their colours, ages, locations, and orbits. These studies all suggest that the young, disk-like dwarfs which reside in the cluster outskirts and move on radial orbits evolved from gas-rich progenitors while the old, nucleated ones which are more centrally-concentrated and follow circular orbits may have formed similarly to the gas-poor giants. As exemplified by Lisker et al. (2008), Toloba et al. (2009) and Paudel et al. (2010), a stellar population analysis of Virgo gas-poor dwarfs would help elucidate the possible bimodal origins of these galaxies.

### 1.3. Spiral galaxies

Since spiral galaxies generally have two principal components, understanding their formation necessarily involves the consideration of both bulges and disks. Large spiral bulges resemble giant gas-poor galaxies in many ways (Kormendy & Illingworth 1983; Dressler 1987; Andredakis et al. 1995; Jablonka et al. 1996; Xilouris et al. 1999; Falcón-Barroso et al. 2002; Gültekin et al. 2009; MacArthur et al. 2009, hereafter M09), even out to intermediate redshift (MacArthur et al. 2008), so that the formation of such “classical” bulges has long been discussed in terms of monolithic collapse or hierarchical merging (Bender et al. 1992). Alternatively, “pseudo-bulges” may be formed through a radial redistribution of disk material due to torques from a bar and/or spiral arms, a process known as secular evolution (Kormendy & Kennicutt 2004).

Early studies of spiral bulges failed to provide a consistent picture of their formation (e.g., Courteau et al. 1996; Peletier et al. 1999). These discrepant results may reflect a morphological trend in bulge formation mechanism (Balcells et al. 2003; Kormendy & Kennicutt 2004), but this clashes with the existence of exponential bulges across the Hubble sequence (MacArthur et al.

2003). Based on a spectroscopic analysis of late-type bulges, M09 have suggested that no conflict exists between the above studies because the formation signature inferred depends on the means by which bulges are observed. For instance, since secular evolution induces SF (see below), optical images of bulges would likely be biased to younger stellar populations (when present), while spectra can more fully sample the entire stellar content, thereby revealing any underlying classical nature. Unfortunately, M09’s study was limited to only eight galaxies.

The origin(s) of spiral bulges should be testable, in principle, through these galaxies’ stellar populations. In the classical bulge formation scenario, a gas disk would accrete around the assembled bulge, thereby making the bulge older and more enriched than the disk; that is, one expects to find negative age and metallicity gradients within such galaxies. On the other hand, the redistribution and scattering of disk stars into a pseudo-bulge would make it appear roughly coeval and isometallic with respect to its (parent) disk; that is, one would expect flat stellar population gradients within these galaxies. Although secular evolution also redistributes the gas of the disk and likely turns it into stars, it is unclear what effect (if any) this will have on a galaxy’s stellar population gradients as the gas should end up spatially confined to a nucleus and rings (Kormendy & Kennicutt 2004). In spite of this, it is clear that important constraints on spiral galaxies’ formation may be obtained by identifying the relative ages and metallicities of their bulges and disks.

Spiral galaxies’ stellar population gradients also reflect on their disk formation. In the traditional scenario (Fall & Efstathiou 1980), disks form inside-out through the collapse of a rotating gas cloud, such that their resulting age and metallicity gradients should both be negative. Simulations and observations both suggest that an outside-in formation scenario, while physically plausible, ought to be rare (Sommer-Larsen et al. 2003; Muñoz-Mateos et al. 2007). A spiral disk stripped of its gas, however, may appear like it formed from outside-in since it should exhibit a positive age gradient (its metallicity gradient would still be negative though) (Boselli et al. 2006). The possible evolution of disks due to environment is thus an important element in the analysis of clusters spirals’ stellar populations. This is supported by the relative paucity of star-forming systems in regions of high density (Dressler 1980), the existence of red disks at  $z \sim 1$  (Koo et al. 2005), and the dependence of the star formation histories of Virgo spirals on their neutral gas deficiencies (Gavazzi et al. 2002).

Although the possible impact of environment on the evolution of cluster spirals is *a priori* unknown, most evidence to date seems to favour hydrodynamic over tidal effects (Boselli & Gavazzi 2006). For instance, observations of neutral gas displaced from the disks of many Virgo cluster spirals suggest that their gas deficiencies result from ram pressure stripping (Chung et al. 2009). Distinguishing between hydrodynamic and tidal effects via the radially-resolved stellar populations of gas-rich cluster galaxies is however not trivial as both are expected to leave a galaxy with

a young central stellar population (Moore et al. 1996; Vollmer et al. 2001). Further complicating this issue is the fact that the popular scenario of SF being quenched within gas-rich galaxies upon their entry into dense environments due to gas removal is not strictly true for cluster galaxies (Gavazzi et al. 1991). Such deviant behaviour may arise if the gas removal mechanism(s) can actually trigger SF via ISM compression. Diagnosing the formation and/or evolution of spiral galaxies based on stellar population data alone may thus be challenging.

## 1.4. Outline

The study of stellar populations is central to understanding galaxy formation and evolution. Broadband colours remain the most efficient means for studying the stellar populations of large galaxy samples. For this, a wide and well-sampled wavelength baseline is optimal for the modeling of galaxy colours (e.g., Gavazzi et al. 2002); the use of optical and near-infrared (NIR) imaging alone already overcomes the age-metallicity degeneracy at optical wavelengths (Cardiel et al. 2003). In this paper we use a large, morphologically complete database of optical and NIR photometry for cluster galaxies (Paper I), down to  $M_B \gtrsim -15$  mag, to study the stellar populations of Virgo cluster galaxies. This database combines imaging from the SDSS (Adelman-McCarthy et al. 2007, 2008), 2MASS (Skrutskie et al. 2006), GOLDMine database (Gavazzi et al. 2003) and our own H-band observations (Paper I).

The layout of this paper is as follows: In §2 we discuss our approach to interpreting the colour gradients of Virgo galaxies (Paper I) with stellar population models. In §3 we extract stellar population profiles and diagnostics for these galaxies to understand their star formation histories (SFHs), chemical evolution, and the parameters that govern them. We interpret these results in §4 as constraints for the formation and evolution scenarios of basic galaxy types (gas-poor giants and dwarfs, and spirals). We conclude in §5 with a summary of major results. Throughout this paper, we express metallicity,  $Z$ , on a logarithmic scale relative to the solar value ( $Z_\odot = 0.02$ ) and assume a distance of 16.5 Mpc to all Virgo cluster galaxies (Mei et al. 2007). We also refer to both S0 and S0/a galaxy types simply as “S0”.

## 2. STELLAR POPULATION MODELING

This study uses the technique of stellar population synthesis to infer the stellar population properties of Virgo galaxies based upon their colour profiles (Paper I). In so doing, we adopt the approach of (MacArthur et al. 2004, hereafter M04), providing references where appropriate for the sake of brevity.

## 2.1. Choice of model and fitting procedure

The simplest use of stellar population synthesis involves the comparison of galaxy colours to predictions for the passive evolution of a coeval, isometallic population of stars (a “simple stellar population”, SSP) to determine light-weighted SSP-equivalent ages and metallicities for the observed stellar populations. Of the several public SSP models we prefer those of Charlot & Bruzual (2010, in preparation; hereafter CB10) for their revision to the treatment of thermally-pulsating AGB (TP-AGB) stars from the preceding version of their models (Bruzual & Charlot 2003)<sup>2</sup>. Although efforts to improve the TP-AGB treatment in stellar population models, like those of CB10, may be inadequate (Conroy & Gunn 2010), our results are essentially invariant under either Bruzual & Charlot (2003) or the CB10 models, as demonstrated in Fig. 1. Other than the TP-AGB issue, competing SSP models differ primarily in details which do not result in significant discrepancies in predicted galaxy colours (M04), though careful examination of the systematic uncertainties in SSP models have only recently begun in earnest (e.g., Conroy et al. 2009).

Rather than assume that the stars in Virgo galaxies came from single bursts of SF (as implicit in the SSP description), we model their colours with synthetic populations from an extended SFH. A single-burst SFH not only conflicts with the idea of hierarchical galaxy growth but there is also much evidence that an SSP is a poor representation of the stellar content of any galaxy, even the reddest spheroids (Serra & Trager 2007; Rogers et al. 2008; Smith et al. 2009; but see Allanson et al. 2009). We opt to model SFHs with simple functional forms, thereby neglecting any possible stochasticity in the SF process (Lee et al. 2007). While the combination of simple SFHs, observational errors and systematic model uncertainties guarantees that our estimated ages and metallicities are not absolutely accurate, our homogeneous approach to modeling Virgo galaxy colours ensures that these estimates are meaningful in a relative sense (Bell & de Jong 2000).

We compute the colours of a composite, isometallic stellar population model via the convolution of SSP spectra of many different ages with a chosen SFH (see Eq. 5 of M04), assuming that SF began 13 Gyr ago. We do not invoke any chemical evolution in our models as this process involves complicated poorly understood astrophysics (Somerville & Primack 1999). Instead, we interpolate between the colours from the metallicity basis set of the CB10 models to create a fine metallicity grid. Our models also do not include any treatment of dust attenuation, for reasons discussed in M04, Paper I and the appendix.

In the spirit of M04, we have explored several stellar population models corresponding to the

---

<sup>2</sup>When present, TP-AGB stars dominate a galaxy’s infrared emission (Maraston 2005) and thus significantly affect its optical-NIR colours (Bruzual 2007; MacArthur et al. 2010).



following SFHs: constant, delayed, exponential, linear, and single-burst. The essential information for all models is summarized in Table 1 and Figure 2; the formulae representing the star formation rate and mean age in each model are quoted in columns 2-3 of the table, while the range in model parameters (star formation timescale/mean age) are given in columns 4-5. The mean age of a given stellar population model is computed from Eq. 10 of M04. Despite assuming an extended SFH for Virgo galaxies, our modeling is still light-biased, such that the fits we obtain may not be representative of a galaxy’s true stellar population if a recent SF burst ( $<1$  Gyr old) has occurred (de Jong & Davies 1997; Serra & Trager 2007; M09). However, M04 demonstrated that such a scenario shrinks the colour coverage of the stellar population models so much as to be inconsistent with observations, unless the burst is small by mass ( $\leq 10\%$ ) and/or heavily obscured by dust.

Since we can only hope to quantify relative differences in the stellar populations of Virgo galaxies, we opt for a single SFH in our modeling. The best choice of SFH is then the one for which the colour coverage is wide enough to match that of as many galaxies in our sample as possible. The SFH colour coverages shown in Figure 2 are compared against each other in Figure 3. While the star formation rates in most models decline with time, the time of peak SF in the delayed and exponential models is variable, such that only they can reproduce the very blue optical colours found in many Virgo gas-rich galaxies (Paper I). For consistency with M04, we adopt the exponential SFH model but, as shown in Figure 4, this choice has little effect on our inferred mean ages and metallicities.

We determine the age and metallicity for the stars of a given radial bin through an explicit grid search for the combination which minimizes the model–data colour residuals. The  $\chi_r^2$  estimate for the fit includes error contributions from calibration, sky, and shot noise uncertainties. For each fit, the model-data normalization is determined from a weighted mean of their differences in the *griH* bands (Eq. 16 of M04), while the age and metallicity errors are estimated from the envelope about the 68 most reliable solutions from fits to 100 Monte Carlo realisations of the measured errors (assuming a normal distribution for each). Our error estimates also flag outlier bins, as their fits will correspond to the edge(s) of the model grid, with zero associated error. We also compute the  $\Delta\chi_r^2 \leq 1$  age-metallicity envelopes about the  $\chi_r^2$  minima for all fits and use their sizes as weights when determining the age and metallicity gradients of Virgo galaxies via linear fits to their stellar population profiles.

### 3. RESULTS

We now consider the age and metallicity profiles of Virgo galaxies, and scaling relations between diagnostics of their stellar populations (age, metallicity, and their gradients) and their structural and environmental parameters. These data are not only sensitive to the relative formation

epochs of different regions in galaxies (e.g., bulge versus disk) but also to the physical mechanisms that control their SFHs and chemical evolution. We interpret these data in terms of the formation and evolution of basic galaxy types in §4.

### 3.1. Age and metallicity profiles

We show in Figure 5 the typical radial age variations for Virgo galaxies, binned by morphological type, where the solid and dashed lines represent the median stack and rms dispersion, respectively, of the individual age profiles in each morphological bin. Having radially binned our galaxies’ light profiles (Paper I) before applying stellar population models to them, we note that the median age profile for each galaxy type extends to at least  $2.0 r_e$  (where  $r_e$  represents the  $H$ -band effective radius) at a minimum signal-to-noise ratio of ten. Table 2 lists the median age gradient (columns 2-4) and central age (column 5) for each morphological bin (with column 6 providing the number of galaxies in each bin), both of which largely reflect our impressions from Figure 5.

We find from Figure 5 that the most galaxy types (E–Sd, dE/dS0, ?) have old central mean ages (9–10 Gyr), while gas-rich dwarfs (Sdm+Sm, Im+BCD) and peculiars (S?) are considerably younger (5–7 Gyr). A bimodality seems apparent in the age gradient distribution for Virgo galaxies, whereby the different galaxy types have either flat (dS0, S0, Sa–Sb) or positive (dE, E, Sbc+Sd, Sdm+Sm, Im+BCD, S?+?) median age gradients (a negative median age gradient is only found in Scd–Sd spirals); note that the age gradient distributions for the dS0, S0, and Sa–Sb galaxy types actually encompass both positive and negative values (Table 2). The gas-rich dwarfs and peculiars have the steepest median age gradients of all galaxy types, which we attribute to their ongoing SF, particularly within their central regions. We speculate that the age upturns in the outskirts of the median age profiles for the Sbc–Sd galaxy types may represent inner disk stars that were scattered outward by spiral arms (Debattista et al. 2006; Foyle et al. 2008; Roškar et al. 2008) or gas stripped disks. Finally, despite having similar median age gradients (when measured in terms of  $r_e^{-1}$ ), Kolmogorov–Smirnov (KS) tests reveal that the age gradient distributions of the gas-poor dwarfs and giants are in fact dissimilar.

The median metallicity profiles of Virgo galaxies are shown in Figure 6, while the median metallicity gradients and central metallicities for all morphological bins are listed in Table 3 (the structure of which is identical to Table 2). The median metallicity profiles of Virgo galaxies are more uniform than their age profiles in the sense that all galaxy types, in the median, exhibit a negative metallicity gradient, albeit spread over a considerable range from  $\sim -0.06 \text{ dex } r_e^{-1}$  for S0’s to  $\sim -0.68 \text{ dex } r_e^{-1}$  for Im’s. Interestingly, the median  $\text{dlog}(Z/Z_\odot)/\text{d}r$  amongst S0–Sd galaxies seems to correlate with morphology, such that later types have more negative gradients, a fact confirmed through KS tests of their gradient distributions. On the other hand, the central metallicities of

Virgo galaxies appear to segregate the different galaxy types into either metal-rich [ $\log(Z_0/Z_\odot) > -0.1$  dex; E–Scd] or metal-poor [ $\log(Z_0/Z_\odot) < -0.2$  dex; dS0/dE, Sm, Im+BCD, S?+?] groups, consistent with brighter (more massive) galaxies tending to be more enriched than the dimmer (less massive) ones (Zaritsky et al. 1994; Tremonti et al. 2004). The latter point is also supported by KS tests which yield a probability less than  $\sim 10\%$  that the gas-poor dwarfs and giants have similar metallicity gradient distributions. However, the low central metallicities of the gas-rich dwarfs, coupled with their steepest of all metallicity gradients, suggests that these galaxies are less enriched than the gas-poor dwarfs, as expected from studies of the Local Group (Grebel et al. 2003).

Knowledge of the typical stellar population gradients within galaxies of all types enables an interpretation of the source(s) of their colour gradients. Comparing the median age, metallicity, and colour (Paper I) profiles of Virgo galaxies, we find that the colour gradients of most galaxy types primarily reflect the outward decrease in their metallicities, save for a few notable exceptions. For one, the negative colour (bluing outward) gradients in Scd+Sd spirals are created by both their negative age and metallicity gradients, while the outward reddening seen in gas-rich peculiar (S?) galaxies is undoubtedly due to their positive age gradients. On the other hand, the positive age and negative metallicity gradients found in E, Sdm+Sm, and BCD galaxies couple so as to generate their quasi-flat colour profiles. Therefore, the null colour gradients within galaxies should not be taken as a reflection of a stellar population with constant age and metallicity profiles.

### 3.1.1. *Comparison with literature*

As in Paper I, we compare our results with similar published studies. The most studied galaxy types in the context of stellar populations is by far the gas-poor giants. Qualitatively speaking, several studies have reported both positive (La Barbera et al. 2010; Tortora et al. 2010) and flat (Franx et al. 1989; Kim & Ann 1990; Saglia et al. 2000; Tamura & Ohta 2003; De Propris et al. 2005; Wu et al. 2005) age gradients within giant gas-poor galaxies, similar to what we have found in the median for Virgo E’s and S0’s, respectively. In addition, these studies unanimously show that these galaxy types possess negative metallicity gradients, spread over a range from  $\sim -0.2$  to  $\sim -0.4$  dex per decade radius. Our measured median metallicity gradient for Virgo giant gas-poor galaxies,  $-0.33$  dex per decade radius, falls nicely within this range.

For the remaining galaxy types (dwarfs and spirals), the literature appears short of quantitative estimates of their stellar population gradients. Any comparison of with our results must be kept strictly qualitative. Despite this limitation, there exists studies of spiral galaxies that report age and metallicity gradients which span a range of positive to negative values (de Jong 1996, M04, Moorthy & Holtzman 2006, Jablonka et al. 2007, M09), as is the case with our Virgo spi-

als. Age and metallicity gradients have been inferred in dwarf galaxies as well (Chilingarian et al. 2007; Chilingarian 2009; Koleva et al. 2009; Paudel et al. 2011), in qualitative agreement with our results.

### 3.2. Stellar population scaling relations

We can also use stellar population gradients of Virgo galaxies to investigate the possible role of galaxy structure and environment in setting radial variations in their SFHs and chemical evolution. As probes of structure, we have used the NIR parameters of concentration ( $C_{28}$ ), apparent magnitude ( $m_H$ ), effective surface brightness ( $\mu_e$ ) and effective radius ( $r_e$ ). For correlations with environment, we have used (projected) cluster-centric distance ( $D_{M87}$ ), local galaxy density ( $\Sigma$ ), and HI gas deficiency ( $Def_{HI}$ ). The definitions and sources of these parameters are provided in Paper I. The age and metallicity gradients of Virgo galaxies are plotted in Figures 7-9 against the above parameters. In each figure, the galaxies are separated into basic groups corresponding to gas-poor (top-left), spiral (top-right), and irregular (lower-left) types, while the distributions of all three groups are superimposed at lower-right. For each group we show the median trend and its rms dispersion (solid and dashed lines, respectively), as well as the typical error per point and the Pearson correlation coefficient,  $r$ . These figures highlight that both structure and environment play little role in the stellar population gradients of Virgo galaxies.

A similar set of plots, but in terms of the effective ages and metallicities, of Virgo galaxies, is presented in Figures 10-12. As a tracer of local SFH and chemical evolution, we define the effective age,  $\langle A \rangle_{\text{eff}}$ , and metallicity,  $Z_{\text{eff}}$ , of a galaxy to be the value of these quantities at its effective radius. We now discuss the scaling relations of the above stellar population diagnostics for each galaxy group.

#### 3.2.1. Gas-poor galaxies

As mentioned above, we do not detect any structural or environmental trends in the stellar population gradients of Virgo gas-poor galaxies. Chief amongst these absentee trends is that the metallicity gradients of Virgo dE/dS0's are independent of luminosity, since Spolaor et al. (2009) found a linear relation between these parameters for systems with masses  $\lesssim 3.5 \times 10^{10} M_{\odot}$  ( $m_H \gtrsim 9.5$  mag at the distance of Virgo; Gavazzi et al. 1996). However, the relatively small number of low-mass galaxies in those authors' sample (13) undermines the reliability of their result. Indeed, the existence of this correlation is far from settled in the literature (De Propris et al. 2005; Michard 2005; Ogando et al. 2005; La Barbera et al. 2010; Tortora et al. 2010). For instance, with

a slightly larger sample, Koleva et al. (2009) showed that gas-poor dwarfs are highly scattered in the metallicity gradient–velocity dispersion (–luminosity) plane, not unlike what we find for the Virgo dE/dS0’s. The observed scatter in metallicity gradient for Virgo dE/dS0’s with  $m_H > 11.0$  mag ( $>0.4$  dex) cannot be explained by observational errors ( $\lesssim 0.2$  dex).

The ages of Virgo gas-poor galaxies also seem to be independent of their structure or environment (but see §3.2.2). The most intriguing of these null results are those involving the parameters  $m_H$  and  $\Sigma$ . Many studies report that the central ages of E/S0’s correlate with both their central velocity dispersion and local galaxy density (Caldwell et al. 2003; Nelan et al. 2005; Thomas et al. 2005; Clemens et al. 2006; Smith et al. 2007). Further, a similar age trend exists for such galaxies against stellar mass indicators (Gallazzi et al. 2005) (but see Graves et al. 2009a,b and Smith et al. 2009); likewise, the integrated ages of Virgo E’s may increase with their  $H$ -band luminosity (Gavazzi et al. 2002). The absence of the above trends persists even when we consider individual morphologies of gas-poor galaxies. We return to this topic in §4.1.3.

The metallicities of Virgo gas-poor galaxies exhibit positive correlations against their structural parameters of  $C_{28}$ ,  $m_H$ , and  $\mu_e$ . The most statistically significant of these trends, that against  $m_H$ , reflects the known metallicity–luminosity relation of galaxies (Zaritsky et al. 1994) and corroborates a similar correlation in terms of these galaxies’ integrated metallicities (Gavazzi et al. 2002). The steepness of our observed  $Z_{\text{eff}}-m_H$  trend, and the contribution of all gas-poor types to it, suggest that the chemical enrichment of these galaxies depends principally on their stellar masses and supports the idea that the galaxian red sequence is due to metallicity variations (Faber 1973; Strateva et al. 2001; Bell et al. 2004; Faber et al. 2007). Contrary to the above trends, the metallicities of Virgo gas-poor galaxies do not correlate with any of their environmental parameters. This result conflicts with the  $Z-\Sigma$  trend (Thomas et al. 2005); we also return to this issue in §4.1.3.

### 3.2.2. *Spirals*

None of the stellar population diagnostics for Virgo spiral galaxies exhibit significant correlations with their structural parameters. One worth noting is the null trend between age and surface brightness. However, Bell & de Jong (2000) and M04 both found a positive correlation between these quantities for field spirals, suggesting that the local potential regulates the SF in those galaxies. An obvious cause for the absence of this trend in our data is that our sample is drawn from a galaxy cluster, whereby environmental effects, such as gas stripping, could perturb the Virgo spiral SFHs (see below). Dust could also skew the age estimates for some of our galaxies.

The ages of Virgo spirals are most strongly affected by their environment, such that galaxies with a greater neutral gas deficiency tend to have older stellar populations. Although Gavazzi et al.

(2002) showed that  $Def_{HI}$  also affects these galaxies’ *integrated* ages, this is secondary to the effect of  $m_H$ , contrary to our results. Also intriguing is the fact that we do not find a  $Def_{HI}$  trend amongst any of the other stellar population diagnostics for Virgo spirals, which would have been expected given the gas deficiency dependence of their local SFHs. For example, the traditional picture of gas stripping posits that the SF in disk outskirts should be truncated before that in the inner regions (Vollmer et al. 2001), thereby changing that galaxy’s age gradient. We return to this discrepancy in §4.3.3. It should finally be noted that while a significant  $Def_{HI}$ -morphology correlation exists amongst Virgo spirals ( $r = -0.68$ ; Paper I), these galaxies alone do not drive the  $Def_{HI}$  trend observed in Figure 12.

### 3.2.3. *Irregulars*

Akin to Virgo spirals, the ages of Virgo irregulars positively correlate with their gas deficiencies (Figure 12), such that systems with larger  $Def_{HI}$  are typically older. Again, though, this trend is surprising given that the metallicities plus age and metallicity gradients for the Virgo irregulars bear no  $Def_{HI}$  imprint. Other than an age-gas deficiency trend, the Virgo irregulars collectively exhibit no other significant correlations in their stellar population diagnostics. The metallicities of Virgo peculiars (S?+?) though, increase with both their luminosities and surface brightnesses (Pearson  $r = +0.66$  and  $+0.48$ , respectively), similar to what was found for Virgo gas-poor galaxies.

## 3.3. Integrated stellar populations

The stellar population scaling relations that we have discussed above apply to the SFHs and chemical evolution of Virgo galaxies on local scales. It is clearly of interest if these correlations also hold on galaxy-wide scales. To explore this, we must look at the integrated characterizations of our galaxies’ stellar populations. Figure 13 shows that the integrated ages and metallicities of Virgo galaxies against their corresponding effective quantities are remarkably consistent with one another. On the other hand, substantial scatter exists between these galaxies’ integrated and effective metallicities, which increases to low  $Z_{eff}$  and is preferentially directed to lower  $Z_{int}$ . Despite this scatter, our galaxies are distributed in a rather monotonic fashion in the  $Z_{int}$ - $Z_{eff}$  plane. The integrated and effective stellar population estimates of Virgo galaxies thus agree with one another (at least in a relative sense), implying that their local scaling relations should apply globally as well.

## 4. DISCUSSION

Below, we discuss the stellar population information of Virgo cluster galaxies in the context of popular galaxy formation and evolution scenarios (i.e., monolithic collapse, hierarchical merging, and secular and environmental evolution; Larson 1974; Cole et al. 2000; Kormendy & Kennicutt 2004; Boselli & Gavazzi 2006) with the aim of establishing which one, or any combinations thereof, contributed most significantly to the inferred stellar content of each basic galaxy type. In this discussion, we focus only on those galaxies for which our sample is richest: gas-poor giants and dwarfs (E/S0 and dE/dS0, respectively), and spirals (Sa–Sd).

### 4.1. Giant gas-poor galaxies

#### 4.1.1. *Monolithic collapse versus hierarchical merging*

As reviewed in §1.1, spectroscopic studies of gas-poor giants have revealed downsizing trends in their central stellar populations which match monolithic collapse scenario predictions more readily than with hierarchical merging. While hierarchical models may be tweaked to reproduce said trends (e.g., De Lucia et al. 2006), many studies have instead contrasted the above scenarios through the stellar population gradients that they predict in E/S0’s (Kobayashi & Arimoto 1999; Tamura & Ohta 2003; Michard 2005; Ogando et al. 2005; Wu et al. 2005; Sánchez-Blázquez et al. 2007; Koleva et al. 2009; Spolaor et al. 2009; Tortora et al. 2010), but there is no consensus. From the perspective of stellar populations, the the formation of gas-poor giants remains open to interpretation.

In order to explain the large central  $[\alpha/\text{Fe}]$  ratios found in local E’s (Thomas et al. 1999), a monolithic-like formation of these galaxies should have happened on a timescale of  $\sim 1$  Gyr. Such a timescale implies shallow, positive age gradients, and steep and negative metallicity gradients on account of the cumulative enrichment of the central regions (Kobayashi 2004; Pipino et al. 2008). Although the recent monolithic collapse models of Pipino et al. (2010) successfully predict our observed metallicity gradients within Virgo E/S0’s ( $-0.33$  dex per decade radius, in the median), their ability to reproduce these galaxies’ age gradients is suspect (A. Pipino, private communication). Also, simulations suggest that the metallicity gradients of collapse remnants should correlate with their stellar masses due to the effect of the potential well on both dissipation and chemo-dynamics during collapse (Kawata & Gibson 2003); we recover no such trend. The stellar population information of Virgo E/S0’s then suggests that these galaxies’ origins were not monolithic-like in nature.

#### 4.1.2. *Merger gas fractions*

Given this tension between stellar population gradients of Virgo gas-poor giants and the monolithic collapse model, let us examine the possibility of a hierarchical origin. At face value, Virgo E/S0's having positive age and negative metallicity gradients are consistent with a scenario whereby their interiors were formed via compact starbursts (Hopkins et al. 2009b), while their outskirts were accreted from (dwarf) satellites (Abadi et al. 2006). That is, these galaxies' stellar population gradients suggest the involvement of both gas-rich and gas-poor mergers in their formation. If this scenario is correct, then the continuous radial increase (decrease) in the age (metallicity) profiles of these Virgo E/S0's contrast with early merger simulations (White 1980) which predicted that violent relaxation would flatten the stellar population gradients in the remnants' outskirts. More recent work has demonstrated, however, that non-negligible age and metallicity gradients, like those in Virgo gas-poor giants, may persist within merger remnants, but only if the progenitors' gradients were roughly twice as steep (Di Matteo et al. 2009; Hopkins et al. 2009c).

Recent photometric studies of Virgo E/S0's have suggested that the gas fractions of the mergers which produced them may be ascertained from the central behaviour (cusp/core) in their light profiles (Côté et al. 2006; Kormendy et al. 2009). That is, gas-rich merger remnants should have cusped light profiles due to their centralized starbursts (Mihos & Hernquist 1996), while gas-poor merger remnants should have cored light profiles due to binary black hole scouring of the central regions (Merritt 2006). Given a cusp/core catalog for Virgo E/S0's (Côté et al. 2006), we can then explore the effect of gas fractions on merger remnants' stellar population gradients. The comparison of the age and metallicity gradients of cusped and cored Virgo E/S0's in Figure 14, suggests that neither of these two galaxy types distinguish themselves in this regard. This bolsters the above claim that progenitors' stellar population gradients may indeed survive merger events.

The stellar population scaling relations of Virgo E/S0's also offer insight into their merger gas fractions. We showed in §3.2.1 that the metallicities of Virgo gas-poor giants increase with both their concentration and luminosity. Although a gas-poor merger of low- $C_{28}$  galaxies could conceivably produce a more concentrated remnant, the absence of merger-induced SF implies that it still would not follow the established  $Z$ - $C_{28}$  relation (i.e., its metallicity would not exceed that of its progenitors). From this, we suggest that a significant fraction of the stellar mass in massive Virgo E/S0's may have formed via starbursts in gas-rich mergers. Coupled with the predominance of cusped light profiles in less luminous Virgo E/S0's (Côté et al. 2006; Kormendy et al. 2009), this indicates that gas-rich mergers play a significant role in the formation of all the gas-poor giants in this cluster.



#### 4.1.3. *Do Virgo E/S0's exhibit downsizing?*

The hallmark of recent spectroscopic studies of local E/S0's is that their central SSP ages and  $[\alpha/\text{Fe}]$  ratios increase with dynamical mass and local density (Caldwell et al. 2003; Nelan et al. 2005; Thomas et al. 2005; Clemens et al. 2006; Smith et al. 2007). However, the authenticity of these downsizing trends remains contentious (Trager et al. 2000; Kelson et al. 2006; Sánchez-Blázquez et al. 2006a; Trager et al. 2008). For instance, Trager et al. (2008) suggest that downsizing may actually represent a mass-dependent trend in the latest central SF episode within these galaxies, since SSP fits are biased by the system's youngest stars. As alluded to in §4.1.1, downsizing has major implications about giant gas-poor galaxy formation. As stated in §3.2.1, we do not detect a statistically significant downsizing trend by stellar mass in the ages of Virgo E/S0's. This result agrees with other conflicting results from prior investigations into the stellar mass dependence of gas-poor giants' stellar populations (Gallazzi et al. 2005; Graves et al. 2009a,b; Smith et al. 2009). Recall also that our non-detection of downsizing refers to the effective radii of Virgo E/S0's, which suggests that these galaxies' integrated SFHs do not downsize with respect to their stellar masses. That is, this result casts doubt on downsizing by mass as a key characteristic of the formation of giant gas-poor galaxies.

We also demonstrated in §3.2.1 that the stellar populations of Virgo E/S0's do not exhibit downsizing trends with environment. While this is, in principle, contrary to the age and metallicity differences between field and cluster gas-poor giants advocated by Thomas et al. (2005), we speculate that our null result may be due to saturation of the Thomas et al. trend on the density scales of galaxy clusters. A plausible source of such saturation may involve the preprocessing of gas-poor galaxies in groups which arrive for the first time into the cluster environment (Mihos 2004). Further exploration of the possible environmental downsizing of Virgo E/S0's will have to await the compilation of accurate distances ( $<10\%$  error) for these galaxies, to enable 3D estimates of cluster-centric distances and local galaxy densities.

#### 4.1.4. *Are S0's a unique galaxy population?*

While most statistical studies of the stellar populations of giant gas-poor galaxies group E's and S0's together (e.g., Thomas et al. 2005), the structural differences between these galaxy types<sup>3</sup> hint at a unique origin for the latter. The origins of S0's have thus been popularly ascribed to an evolution of spiral galaxy progenitors, driven by environment, which involves the removal of the

---

<sup>3</sup>By definition, S0's have dynamically fragile disks and, in Virgo, are on average more concentrated, brighter and larger than E's.

latter’s gas (via hydrodynamic and/or tidal processes) and the subsequent fading of their stellar disks (Boselli & Gavazzi 2006). The increasing fraction of blue cluster galaxies to high redshifts (Butcher & Oemler 1978) is perhaps the strongest evidence in favour of such a scenario. Since a hydrodynamic or tidal transformation of a spiral galaxy should leave its remnant with a central gas reservoir (see below), one would expect to uncover environmental signatures in S0’s stellar populations (e.g., positive age gradients) if this scenario was true. Studies along these lines, however, have so far failed to reveal conclusive results (Chamberlain et al. 2011, and references therein).

The positive age and negative metallicity gradients found in some Virgo S0’s conform with their possible evolutionary origin. Younger and more enriched central regions in galaxies that have experienced either ram pressure stripping or harassment are a generic expectation from simulations of these effects (Moore et al. 1996; Vollmer et al. 2001). These simulations show that remnants of these processes are left with central gas reservoirs due to either the stronger gravitational restoring force in those regions (re: ram pressure stripping), or tidally-induced central gas flows (re: harassment). The participation of Virgo S0’s in the age-gas deficiency trend for the gas-rich systems in this cluster (Figure 12) also supports an evolutionary origin for these galaxies. This trend and the lack of  $D_{M87}$  or  $\Sigma$  signatures in the stellar population diagnostics of Virgo S0’s, strongly suggest that ram pressure stripping would be the preeminent cause of their evolution from a gas-rich spiral progenitor.

Alternatively, Virgo S0’s may have formed, like Virgo E’s, through hierarchical merging. Both the prominence of S0 bulges (Dressler 1980) and the evidence for (small) disks in the light profiles and kinematic maps of classified E’s (Krajnović et al. 2008; McDonald et al. 2009) suggest that these two galaxy types represent a continuum in gas-poor giant structure. Furthermore, the stellar population diagnostics for Virgo E’s and S0’s follow similar scaling relations (see also Jaffe et al. 2010). If Virgo E’s and S0’s share a common origin, as these commonalities suggest, then the positive age gradients we find in many of the latter imply that their disks existed prior to their bulges. While stellar disks can survive a minor merger (Hernquist & Mihos 1995), it is unlikely that such events could build the massive bulges of S0’s. Conversely, major mergers may explain the formation of Virgo S0’s given the simulations (Hopkins et al. 2009a) and observations (Kannappan et al. 2009; Catinella et al. 2010) that both support the idea of disk survival (or even regrowth) after such an event, provided that it is of a high gas fraction. Gas-rich merging may be problematic though as the gas disk must be promptly removed after the merger to keep the disk’s stellar population older than that of the bulge; this problem, of course, does not exist for Virgo S0’s having negative age gradients. Mergers can consume gas through centripetal gas flows and subsequent starbursts (Mihos & Hernquist 1996), but it is unlikely that this mechanism will deplete the remnant’s entire gas disk. Thus, the merger scenario of S0 formation may still require an external agent (e.g., ram pressure stripping) to remove gas from these galaxies’ progenitors; that is, no one mechanism may explain these galaxies’ origins (Bedregal et al. 2008).

## 4.2. Dwarf gas-poor galaxies

The gradual realization that gas-rich and gas-poor dwarf galaxies overlap in terms of their structure, dynamics, gas content, substructure and SFHs (Lin & Faber 1983; Pedraz et al. 2002; Conselice et al. 2003a; Lisker et al. 2006a; Tolstoy et al. 2009) has lent considerable weight to the idea of an evolutionary link between these two galaxy types. External mechanisms that could drive the evolution of a gas-rich dwarf into a gas-poor dwarf include ram pressure stripping or thermal evaporation of its ISM, and galaxy harassment (Gunn & Gott 1972; Cowie & Songaila 1977; Moore et al. 1996). An internal mechanism for such a depletion is unlikely due to dwarf galaxies’ (implied) inefficiencies in both SF (Grebel et al. 2003) and gas expulsion (Mac Low & Ferrara 1999; Weisz et al. 2008; Lee et al. 2009; Tolstoy et al. 2009). Despite the extensive overlap of their physical properties, important differences remain between gas-rich and gas-poor dwarfs in terms of their surface brightnesses, metallicities and globular cluster statistics (Bothun et al. 1986; Grebel et al. 2003; Strader et al. 2006). A primordial origin, like that for gas-poor giants (i.e., monolithic collapse or hierarchical merging), thus remains viable for gas-poor dwarfs, and is supported by the very old ages and low metallicities of the nucleated dwarfs in both the Coma and Fornax galaxy clusters (Rakos & Schombert 2004).

### 4.2.1. A primordial origin?

We have found that a majority of Virgo gas-poor dwarfs in our sample have positive age and negative metallicity gradients (admittedly though, Table 2 indicates that the former are statistically consistent with being flat). Given such a stellar population gradient combination, it seems unlikely that these galaxies could be primordial in origin. For instance, the metallicity gradients in Virgo dE/dS0’s are collectively steeper than those of Virgo E/S0’s, contrary to the predicted flattening of this diagnostic towards low masses in monolithic collapse models (Kawata & Gibson 2003). The absence of such a trend in our data is supported by the Pearson test ( $r = +0.34$ ) shown in the lower-right panel of Figure 7 for Virgo gas-poor galaxies. The primordial origin hypothesis for Virgo dE/dS0’s is also discredited on account that these galaxies do not exhibit comparable stellar population scaling relations with those of Virgo E/S0’s. The stellar population data Virgo dE/dS0’s thus argue against either a hierarchical or monolithic-like origin for them.

### 4.2.2. The evolutionary scenario

Much of the stellar population data for the Virgo gas-poor dwarfs is readily interpreted in the context of an evolutionary origin. While our data cannot confirm which environmental mechanism

is most likely to have removed these galaxies’ gas, the absence of trends in their stellar population diagnostics with both galaxy density and cluster-centric distance disfavors it being harassment. On the other hand, the fact that gas stripping of (more massive) Virgo spiral galaxies is observed (Chung et al. 2009, and references therein) and should increase in efficiency with lower masses makes this mechanism appealing. Given this, negative age gradients in Virgo dE/dS0’s may arise from the strangulation of gas-rich progenitors’ haloes, while positive age gradients may result from ram pressure stripping of progenitors’ gas disks (Boselli et al. 2008).

Not all the stellar population information for Virgo dE/dS0’s agrees with their possible evolutionary origin. While we find broad consistency in the central metallicities of all Virgo dwarfs (Table 3), the young ages of our Im+BCD’s suggests that our (light-biased) estimates sample only their most recently formed stars, such that their fitted metallicities are better thought of as being upper limits. This, coupled with the more negative metallicity gradients within the Im+BCD’s, then implies that the true metallicities of Virgo gas-rich and gas-poor dwarfs are likely discrepant, as found amongst Local Group dwarfs as well (Grebel et al. 2003). The fact that we find mild agreement between the central metallicities of all Virgo dwarfs, however, implies that Im+BCD’s are at least capable of enriching themselves to the same degree as dE/dS0’s. This suggests a solution to discrepant metallicity problem which the evolutionary scenario faces, whereby the progenitors of Virgo dE/dS0’s sufficiently enrich themselves before completely losing their gas supplies (e.g., through triggered SF). This can happen once a dwarf galaxy has been stripped of its gas, as only evolved stars can replenish its ISM at that point (Boselli et al. 2008). Conversely, the extremely metal-poor outskirts in Virgo Im’s may be understood as a recent accretion of pristine gas onto those regions (i.e., those estimates are lower limits). Considering our poor statistics in the stellar population diagnostics of Virgo Im+BCD’s, we refrain from pursuing this comparison further.

In a manner similar to the gas-poor giants, the Virgo dS0’s exhibit several structural differences relative to the Virgo dE’s, suggesting a different origin for these two gas-poor dwarf types. This is supported by KS tests with low probabilities ( $P < 0.5$ ) between their respective stellar population diagnostics. Lisker et al. (2009, and references therein), Toloba et al. (2009), and Paudel et al. (2010) have also explored the idea of distinct classes of Virgo gas-poor dwarfs and argued that the younger, flatter, less centrally clustered population is the prototype for the evolutionary remnant of a low-mass spiral or gas-rich dwarf<sup>4</sup>. These authors also suggest that the older, rounder, more centrally clustered gas-poor dwarfs<sup>5</sup> may have a primordial origin. The many structural and stellar population differences that we find between Virgo dS0’s and dE’s thus bolster the main conclusion of the above studies; namely, that the Virgo gas-poor dwarfs likely formed

---

<sup>4</sup>This population also has the highest frequency of substructure (e.g., bars) and blue centers.

<sup>5</sup>This population also has the highest frequency of nucleation.

through at least two different channels.

### 4.3. Spiral galaxies

As discussed in §1.3, the formation of spiral galaxy bulges remains unsettled, particularly with respect to the relative contributions of hierarchical merging (Bender et al. 1992) and secular evolution (Kormendy & Kennicutt 2004) as a function of Hubble type. Making matters worse, to distinguish these processes is non-trivial as satellite accretion is likely to excite disk instabilities (Gauthier et al. 2006). Furthermore, while the formation of spiral galaxy disks is well understood in principle as the self-gravitating collapse of a rotating gas cloud (Fall & Efstathiou 1980), the local environment may play a significant role in the evolution of this component in cluster spirals. Below, we try to understand the formation of the bulges and disks of Virgo spirals via comparisons of their relative ages and metallicities and assuming that bulge light dominates these galaxies’ interiors ( $\lesssim 1 r_e$ ). Decompositions of Virgo spirals’ light profiles indeed show that the bulge-to-total light ratio is typically above 50% within their effective radii (McDonald et al. 2009).

The negative metallicity gradients found in most Virgo spirals indicates that their bulges are more enriched than their disks. Conversely, the age gradients in Virgo spirals range from being typically positive for early-types (Sa-Sbc) to negative for late-types (Scd+Sd). Each spiral (sub-)class, however, contains a mixture of positive and negative age gradients (Table 2), such that no one scenario can describe the origin of any one galaxy type. We therefore address the origins of Virgo spirals based on age gradient sign rather than morphological type. The definite existence of positive and negative age gradients in these systems is confirmed by their measured error envelopes which do not typically overlap with zero.

#### 4.3.1. Positive age gradients

The combination of a young, metal-rich bulge and an old, metal-poor disk (found in  $\sim 35\%$  of Virgo spirals, most commonly Sa–Sc’s) suggests a formation scenario for the bulge which involves the accumulation of a central gas reservoir. Both secular evolution and a recent gas-rich minor merger<sup>6</sup> could create such a reservoir (Pfenniger & Norman 1990; Hernquist & Mihos 1995). However, the former scenario would likely fail to produce a positive age gradient for two reasons. First, the gas reservoir that a bar creates via a centripetal flow from the disk would be spatially confined to the galaxy’s nucleus and not spread over the entire bulge. Second, the scat-

---

<sup>6</sup>We stipulate that such a merger must be of a low mass ratio if the (old) disk is to survive such an event.

tering of stars into the pseudo-bulge by a bar should actually flatten a spiral galaxy’s age gradient (Kormendy & Kennicutt 2004). Secular evolution is thus unlikely the source of positive age gradients in Virgo (early-type) spirals.

While secular evolution may fails to explain the positive age gradients in Virgo spirals, the success of the gas-rich minor merger scenario is contingent upon at least two constraints. First, some mechanism is needed to restrict the funneling of gas into the nucleus as this will not likely lead to the creation of a positive gradient over a large radial extent within the remnant. This funneling may derive from the weak torques acting on the gas during a minor merger (Hopkins et al. 2009a) or from tidal disruption of the secondary before coalescence, such that the merger turns into an accretion event. Second, the merging of a gas-rich dwarf with a spiral galaxy should create a positive metallicity gradient, due to the deposition of metal-poor gas and stars into the bulge. This challenge for the merger scenario may be overcome if the accreted gas has either been pre-enriched or is consumed over a long timescale.

Although gas-rich minor mergers may explain the origin of bulges in Virgo spirals with positive age gradients, it offers no insight as to why stellar ages and metallicities continue to increase and decrease, respectively, outward in these galaxies’ disks. The most compelling scenarios for the creation of such disks include outside-in formation and disk fading, wherein the latter occurs after depletion of the gas disk by external agents. While the formation of outside-in disks has been seen in simulations (Sommer-Larsen et al. 2003), current observational evidence suggests that this is a rare mechanism for the growth of spiral disks (Muñoz-Mateos et al. 2007). Therefore, the existence of positive age gradients in most Virgo bulges and disks in our sample may be explained by a combination of gas-rich minor merging and disk fading. We shall revisit the topic of gas disk depletion in §4.3.3.

#### 4.3.2. *Negative age gradients*

The alternate combination of an old, metal-rich bulge with a young, metal-poor disk (found in  $\sim 35\%$  of Virgo spirals, most commonly Sc–Sd’s) implies that the gas supply of the disk accumulated later and/or was converted to stars over a longer timescale than that of the bulge (i.e., the bulge formed before the disk). Bulges may deplete their gas supplies most efficiently at early epochs, thereby making them relatively old, by undergoing major mergers. This suggestion contradicts the popular wisdom that late-type spirals possess pseudo-bulges Balcells et al. (2003); MacArthur et al. (2003); Kormendy & Kennicutt (2004), but recent spectroscopic stellar population analyses have shown that the stellar masses of late-type bulges are indeed predominantly old (M09; Saglia et al. 2010), as expected in a classical sense. Also, the existence of a negative age gradient in a spiral galaxy that has experienced the stellar mixing and radial gas flows associated

with secular evolution seems counter-intuitive. The bulges of such galaxies are then most consistent with having originated through mergers.

A negative age gradient throughout a spiral galaxy also places constraints on the formation mechanism and epoch of its disk. Such radial behaviour in stellar age, coupled with a negative metallicity gradient, suggests that the outskirts of these galaxies were formed through a more extended SFH, from a more pristine ISM and suffered metal-rich outflows, while their central regions would have resulted from a more intense but short-lived SFH which involved substantial gas recycling. Such an inside-out origin of Virgo late-type disks agrees well with results from  $\Lambda$ CDM simulations of disk formation (Mo et al. 1998; Sommer-Larsen et al. 2003) and supports the idea that the gravo-thermal collapse of gas clouds within them (and thus their star formation rates) depends on the local surface mass density (Kennicutt 1989). The fact that the disks in Virgo late-type spirals are younger than their bulges also suggests that these gaseous disks have not yet (or only recently) been stripped by the Virgo ICM. If true, then these galaxies are likely recent additions to this cluster.

#### 4.3.3. *Gas stripping*

The existence of positive age gradients and a statistically significant age- $Def_{HI}$  scaling relation in Virgo spirals both argue that gas removal plays a fundamental role in the evolution of these galaxies. We ascribe the agent of gas removal to ram pressure since several observational evidences favour its influence on gas-rich cluster galaxies (for a summary, see Chung et al. 2009, and references therein), its efficiency at quenching the SF in spiral disks is high (Poggianti et al. 1999; Roediger & Hensler 2005; Kronberger et al. 2008), and the ages of Virgo spirals are evidently independent of both their cluster-centric distances and local galaxy densities<sup>7</sup>. Although cluster galaxies are expected to quickly lose their gas haloes to hydrodynamical interactions at large cluster-centric radii (Balogh et al. 2000; Bekki et al. 2002; Murphy et al. 2009), such a strangulation scenario (Larson et al. 1980) should not produce positive age gradients within them if the local star formation rate is density-dependent (M04).

The removal of a cluster spiral’s gas supply should not only affect its SFH, but other factors related to its stellar populations as well. Ram pressure stripping gradually removes a spiral galaxy’s gas disk from the outside-in (Vollmer et al. 2001), but the deeper potential well towards its center prevents the complete loss of its HI supply, ultimately leaving it with a large anemic annulus about

---

<sup>7</sup>However, projection effects in the diagnostics  $D_{M87}$  and  $\Sigma$  and the possibility that ram pressure stripping can occur at large cluster-centric radii in Virgo due to a dynamic or “lumpy” ICM (Crowl & Kenney 2008) may also be playing a role in generating these null results.

its center. Given such a range in the gas retention properties within cluster spirals, the age gradient of a highly deficient system might be expected to be more positive than that of a less deficient system, since SF will undoubtedly be quenched in the former’s outer disk but not in its central regions. Moreover, if SF is quenched in a galaxy’s outskirts, so too should the enrichment of the local ISM, such that highly deficient spirals should be more metal-poor and have more negative metallicity gradients than less deficient spirals. Finding no  $Def_{HI}$  effect whatsoever on either the metallicities or the stellar population gradients of Virgo spirals is thus disconcerting. Many factors may contribute to wash out these trends, however, such as a rapid stripping timescale, a recent stripping epoch for the highly deficient spirals, and/or triggered SF or gas fallback accompanying the stripping event (as seen in simulations; Vollmer et al. 2001). The absence of  $Def_{HI}$  trends expected in the stellar population diagnostics of cluster spirals may be evidence that gas stripping does not simply entail a gradual outside-in removal of their gas and subsequent quenching of their SF.

To bolster our claim that the effects of gas stripping on cluster spirals is more complex than the simple (intuitive) picture described above, we show in Figure 15 the stellar population profiles for Virgo spirals that we have in common with (Crowl & Kenney 2008, ; hereafter CK08). CK08 analysed the stellar populations located just beyond the truncated  $H\alpha$  disks in several Virgo spirals to determine when SF was quenched in those regions. They concluded that the highly HI-deficient galaxies must have lost their gas disks recently ( $\leq 500$  Myr) without any triggering of SF. Seven of CK08’s spirals overlap with our sample, thereby enabling a qualitative comparison of our age profiles with them. We find that the age profiles of only two of these galaxies (VCC0873 and VCC1126) notably increase beyond their  $H\alpha$  disks, implying that their disks were stripped gradually, not recently. Interestingly, the age profile of VCC1690 ( $Def_{HI} = 1.07$ ) actually decreases just beyond its  $H\alpha$  disk, suggesting that ram pressure has actually triggered SF during the stripping process. The age profiles of the other four galaxies remain flat beyond their  $H\alpha$  disks, implying that these galaxies were instead stripped rapidly. The age profiles for Virgo spirals and our comparison with CK08 suggest that the gas stripping timescales for gas-rich galaxies falling into the Virgo cluster may not be uniform (Poggianti et al. 1999; Vollmer et al. 2001; Roediger & Hensler 2005; Kronberger et al. 2008) and that ram pressure may indeed promote SF in galaxies before ultimately quenching it.

## 5. Conclusions

We have used high-quality optical and near-infrared ( $griH$ ) imaging of  $\sim 300$  Virgo cluster galaxies to determine radial stellar population variations for a representative sample spanning the full range of galaxian parameter space. We have also compared stellar population diagnostics



(ages, metallicities, and their gradients) with structural and environmental parameters to investigate their contribution to galaxies' SFHs and chemical evolution. All these data considered, we have developed plausible formation and evolution scenarios for each of the major galaxy types (gas-poor giants and dwarfs, and spirals) within a cluster setting. Here is a summary of our main results:

- Most galaxies' colour gradients are due to variations in metallicity; ellipticals, Sbc–Sd spirals, gas-rich dwarfs, and peculiars also show non-negligible age variations;
- Although reddening can skew stellar population estimates from colours, realistic dust modelling cannot be achieved through colour information alone;
- Of the SFHs considered, only an exponential SFH can simultaneously account for the wide colour range exhibited by all galaxy types, especially the gas-poor giant galaxies;
- The metallicity gradients of Virgo galaxies become increasingly negative towards later types along the Hubble sequence;
- Significant correlations in the stellar population diagnostics of Virgo galaxies indicate that:
  - the chemical evolution of gas-poor galaxies is determined by the interplay between stellar masses (nucleosynthesis sites) and surface densities (potential well depth),
  - the higher metallicities of E/S0's that experienced more dissipation during their formation suggests that their stellar masses were built up *in situ*,
  - the SFHs of gas-rich cluster galaxies are strongly affected by complicated gas removal processes that likely trigger SF as well as inhibit it.
- The stellar population data for Virgo galaxies suggest the following formation and evolution scenarios for the major galaxy types in this cluster:
  - Giant gas-poor (E/S0) galaxies grew mostly via gas-rich mergers but some gas-poor mergers, as well as gas removal processes in S0's, also likely play a role;
  - Dwarf gas-poor (dE+dS0) galaxies do not result from a single formation mechanism but the dominant production channel likely involves an evolution from a gas-rich progenitor (e.g., Im+BCD) that is driven by environment;
  - Spiral (Sa–Sd) galaxies having a bulge that is older and more enriched than the disk likely formed their bulge through merging and grew their disk inside-out afterward, free from environmental effects. Conversely, spirals with a disk older and less enriched than their bulge, whilst still having a merger-built bulge, likely underwent stripping of their gas disk.

We are grateful to L. P. Chamberlain, C. Conroy, E. Emsellem, L. Ferrarese, and C. Maraston for insightful discussions. This research has made use of the NASA/IPAC extragalactic and GOLDMine databases. J. R. and S.C. acknowledge financial support from the National Science and Engineering Council of Canada.

## 6. APPENDIX: Dust

The presence of dust in galaxies affects broadband studies of their stellar populations since a change in reddening can mimic variations in both age and metallicity (Byun et al. 1994; de Jong 1996). The weak SF characteristics of gas-poor galaxies (Serra & Trager 2007) imply that reddening of their colours by dust should be minimal since their dust reservoirs should not have been recently replenished by stellar feedback (Eminian et al. 2008). The same cannot be said for gas-rich galaxies, as evidenced by the extremely red optical-NIR colours that we find in some Virgo spirals (Paper I); however, MacArthur et al. (2010) show that such red colours could also result from the presence of a significant TP-AGB population. Rather than correct our photometry using idealized dust models (e.g., Gavazzi et al. 2002), we instead address the impact that dust would have on galaxy colours.

To gauge the effect of reddening, we examine three popular dust models: (1) foreground screen, (2) face-on triplex (Disney et al. 1989), and (3) clumpy medium (Charlot & Fall 2000). The screen model follows a simple prescription,  $A_\lambda = 1.08\tau_\lambda$ , where  $A_\lambda$  and  $\tau_\lambda$  are the extinction and optical depth in band  $\lambda$ , respectively. The triplex model assumes exponentially declining distributions of stars and dust in both the radial and vertical directions. We calculate triplex extinctions according to Eq. (14) of M04, which invokes a simple treatment of scattering (de Jong 1996). M04 argued that a large reddening gradient is only achieved with the triplex model when the stellar and dust scale lengths are equal, contrary to observations (Xilouris et al. 1999). For both the screen and triplex models, we use the Milky Way extinction curve and albedos from Gordon et al. (1997). The clumpy medium model mimics the preferential but short-lived extinction of young star clusters (Witt et al. 1992; Gordon et al. 1997) due to the higher dust concentrations in molecular clouds than in the diffuse ISM. The power-law dependence of the extinction curve in this model has been verified in a multi-band study of SDSS galaxies (Johnson et al. 2007). However, as Charlot & Fall contend, the neglected scattering in their model make its applicability to galaxian light profiles questionable. Indeed, the absence of a detailed scattering treatment in most analytic dust models is another valid reason to forego reddening corrections to our data.

We compare in Figure 16 the predictions for each of the above dust models against our preferred exponential SFH model. The predicted reddening mostly affects optical-NIR colours and thus mostly skews metallicity estimates (Bell & de Jong 2000). Considering our typical measure-

ment errors however (Paper I), the models are degenerate with respect to colours and even themselves. Although the dust extinction vectors lie nearly parallel to the median colour gradients of our Virgo spirals (Paper I), unfeasibly large attenuations would be required to fully explain the magnitude of these galaxies' gradients (M04). With exception to a few edge-on Virgo spirals that lie completely redward of the exponential model grid (e.g., VCC0873), we can thus rule out dust as a dominant contributor to the colours of Virgo gas-rich galaxies. This point is supported by our finding in Paper I that these galaxies' central colours are independent of inclination. Constraints on the dust properties of Virgo cluster galaxies should be significantly improved with the highly anticipated completion of several ongoing dedicated X-ray, UV, optical, IR-FIR, and sub-mm surveys of this cluster.

## REFERENCES

- Abadi, M. G., Navarro, J. F., & Steinmetz, M. 2006, *MNRAS*, 365, 747
- Adelman-McCarthy, J. K., et al. 2007, *ApJS*, 172, 634
- Adelman-McCarthy, J. K., et al. 2008, *ApJS*, 175, 297
- Allanson, S. P., Hudson, M. J., Smith, R. J., & Lucey, J. R. 2009, *ApJ*, 702, 1275
- Andredakis, Y. C., Peletier, R. F., & Balcells, M. 1995, *MNRAS*, 275, 874
- Balcells, M., Graham, A. W., Domínguez-Palmero, L., & Peletier, R. F. 2003, *ApJL*, 582, L79
- Balogh, M. L., Navarro, J. F., & Morris, S. L. 2000, *ApJ*, 540, 113
- Barazza, F. D., Binggeli, B., & Jerjen, H. 2002, *A&A*, 391, 823
- Baugh, C. M. 2006, *Reports on Progress in Physics*, 69, 3101
- Bedregal, A. G., Aragón-Salamanca, A., Merrifield, M. R., & Cardiel, N. 2008, *MNRAS*, 387, 660
- Bekki, K., Couch, W. J., & Shioya, Y. 2002, *ApJ*, 577, 651
- Bell, E. F., & de Jong, R. S. 2000, *MNRAS*, 312, 497
- Bell, E. F., et al. 2004, *ApJ*, 608, 752
- Bell, E. F., et al. 2006, *ApJ*, 640, 241
- Bender, R., Burstein, D., & Faber, S. M. 1992, *ApJ*, 399, 462

- Binggeli, B., Tarenghi, M., & Sandage, A. 1990, *A&A*, 228, 42
- Boselli, A., & Gavazzi, G. 2006, *PASP*, 118, 517
- Boselli, A., Boissier, S., Cortese, L., Gil de Paz, A., Seibert, M., Madore, B. F., Buat, V., & Martin, D. C. 2006, *ApJ*, 651, 811
- Boselli, A., Boissier, S., Cortese, L., & Gavazzi, G. 2008, *ApJ*, 674, 742
- Boselli, A., Boissier, S., Cortese, L., & Gavazzi, G. 2008, *A&A*, 489, 1015
- Bothun, G. D., Mould, J. R., Caldwell, N., & MacGillivray, H. T. 1986, *AJ*, 92, 1007
- Bower, R. G., Benson, A. J., Malbon, R., Helly, J. C., Frenk, C. S., Baugh, C. M., Cole, S., & Lacey, C. G. 2006, *MNRAS*, 370, 645
- Bruzual, A. G. 2007, *IAU Symposium*, 241, 125
- Bruzual, G., & Charlot, S. 2003, *MNRAS*, 344, 1000
- Butcher, H., & Oemler, A., Jr. 1978, *ApJ*, 219, 18
- Byun, Y. I., Freeman, K. C., & Kylafis, N. D. 1994, *ApJ*, 432, 114
- Caldwell, N., Rose, J. A., & Concannon, K. D. 2003, *AJ*, 125, 2891
- Cardiel, N., Gorgas, J., Sánchez-Blázquez, P., Cenarro, A. J., Pedraz, S., Bruzual, G., & Klement, J. 2003, *A&A*, 409, 511
- Catinella, B., et al. 2010, *MNRAS*, 403, 683
- Prochaska Chamberlain, L. C., Courteau, S., McDonald, M., Rose, J. A. 2011, *MNRAS*, accepted
- Charlot, S., & Fall, S. M. 2000, *ApJ*, 539, 718
- Chilingarian, I. V., Sil'Chenko, O. K., Afanasiev, V. L., & Prugniel, P. 2007, *Astronomy Letters*, 33, 292
- Chilingarian, I. V. 2009, *MNRAS*, 394, 1229
- Chung, A., van Gorkom, J. H., Kenney, J. D. P., Cowl, H., & Vollmer, B. 2009, *AJ*, 138, 1741
- Clemens, M. S., Bressan, A., Nikolic, B., Alexander, P., Annibali, F., & Rampazzo, R. 2006, *MNRAS*, 370, 702
- Cole, S., Lacey, C. G., Baugh, C. M., & Frenk, C. S. 2000, *MNRAS*, 319, 168

- Conroy, C., Gunn, J. E., & White, M. 2009, *ApJ*, 699, 486
- Conroy, C., & Gunn, J. E. 2010, *ApJ*, 712, 833
- Conselice, C. J., O’Neil, K., Gallagher, J. S., & Wyse, R. F. G. 2003, *ApJ*, 591, 167
- Conselice, C. J., Bershad, M. A., Dickinson, M., & Papovich, C. 2003, *AJ*, 126, 1183
- Côté, P., et al. 2006, *ApJS*, 165, 57
- Courteau, S., de Jong, R. S., & Broeils, A. H. 1996, *ApJL*, 457, L73
- Cowie, L. L., & Songaila, A. 1977, *Nature*, 266, 501
- Crowl, H. H., & Kenney, J. D. P. 2008, *AJ*, 136, 1623
- Debatista, V. P., Mayer, L., Carollo, C. M., Moore, B., Wadsley, J., & Quinn, T. 2006, *ApJ*, 645, 209
- de Jong, R. S. 1996, *A&A*, 313, 377
- de Jong, R. S., & Davies, R. L. 1997, *MNRAS*, 285, L1
- De Lucia, G., Springel, V., White, S. D. M., Croton, D., & Kauffmann, G. 2006, *MNRAS*, 366, 499
- De Propris, R., Colless, M., Driver, S. P., Pracy, M. B., & Couch, W. J. 2005, *MNRAS*, 357, 590
- De Rijcke, S., Dejonghe, H., Zeilinger, W. W., & Hau, G. K. T. 2003, *A&A*, 400, 119
- Di Matteo, P., Pipino, A., Lehnert, M. D., Combes, F., & Semelin, B. 2009, *A&A*, 499, 427
- Disney, M., Davies, J., & Phillipps, S. 1989, *MNRAS*, 239, 939
- Dressler, A. 1980, *ApJ*, 236, 351
- Dressler, A. 1987, *ApJ*, 317, 1
- Dutton, A. A. 2009, *MNRAS*, 396, 121
- Eggen, O. J., Lynden-Bell, D., & Sandage, A. R. 1962, *ApJ*, 136, 748
- Eminian, C., Kauffmann, G., Charlot, S., Wild, V., Bruzual, G., Rettura, A., & Loveday, J. 2008, *MNRAS*, 384, 930
- Emsellem, E., et al. 2007, *MNRAS*, 379, 401

- Faber, S. M. 1973, *ApJ*, 179, 731
- Faber, S. M., et al. 1997, *AJ*, 114, 1771
- Faber, S. M., et al. 2007, *ApJ*, 665, 265
- Falcón-Barroso, J., Peletier, R. F., & Balcells, M. 2002, *MNRAS*, 335, 741
- Fall, S. M., & Efstathiou, G. 1980, *MNRAS*, 193, 189
- Ferrarese, L., et al. 2006, *ApJS*, 164, 334
- Ferrarese, L., et al. 2006, *ApJL*, 644, L21
- Foster, C., Proctor, R. N., Forbes, D. A., Spolaor, M., Hopkins, P. F., & Brodie, J. P. 2009, *MNRAS*, 400, 2135
- Foyle, K., Courteau, S., & Thacker, R. J. 2008, *MNRAS*, 386, 1821
- Franx, M., Illingworth, G., & Heckman, T. 1989, *AJ*, 98, 538
- Gallazzi, A., Charlot, S., Brinchmann, J., White, S. D. M., & Tremonti, C. A. 2005, *MNRAS*, 362, 41
- Gauthier, J.-R., Dubinski, J., & Widrow, L. M. 2006, *ApJ*, 653, 1180
- Gavazzi, G., Boselli, A., & Kennicutt, R. 1991, *AJ*, 101, 1207
- Gavazzi, G., Pierini, D., & Boselli, A. 1996, *A&A*, 312, 397
- Gavazzi, G., Bonfanti, C., Sanvito, G., Boselli, A., & Scodeggio, M. 2002, *ApJ*, 576, 135
- Gavazzi, G., Boselli, A., Donati, A., Franzetti, P., & Scodeggio, M. 2003, *A&A*, 400, 451
- Gavazzi, G., Boselli, A., van Driel, W., & O’Neil, K. 2005, *A&A*, 429, 439
- Gavazzi, G., Boselli, A., Cortese, L., Arosio, I., Gallazzi, A., Pedotti, P., & Carrasco, L. 2006, *A&A*, 446, 839
- Geha, M., Guhathakurta, P., & van der Marel, R. P. 2002, *AJ*, 124, 3073
- Gordon, K. D., Calzetti, D., & Witt, A. N. 1997, *ApJ*, 487, 625
- Graham, A. W., & Guzmán, R. 2003, *AJ*, 125, 2936
- Graham, A. W., Jerjen, H., & Guzmán, R. 2003, *AJ*, 126, 1787

- Graves, G. J., Faber, S. M., & Schiavon, R. P. 2009, *ApJ*, 693, 486
- Graves, G. J., Faber, S. M., & Schiavon, R. P. 2009, *ApJ*, 698, 1590
- Grebel, E. K., Gallagher, J. S., III, & Harbeck, D. 2003, *AJ*, 125, 1926
- Gunn, J. E., & Gott, J. R., III 1972, *ApJ*, 176, 1
- Gültekin, K., et al. 2009, *ApJ*, 698, 198
- Haines, C. P., La Barbera, F., Mercurio, A., Merluzzi, P., & Busarello, G. 2006, *ApJ*, 647, L21
- Hernquist, L., & Mihos, J. C. 1995, *ApJ*, 448, 41
- Hopkins, P. F., Cox, T. J., Younger, J. D., & Hernquist, L. 2009, *ApJ*, 691, 1168
- Hopkins, P. F., Cox, T. J., Dutta, S. N., Hernquist, L., Kormendy, J., & Lauer, T. R. 2009, *ApJS*, 181, 135
- Hopkins, P. F., Lauer, T. R., Cox, T. J., Hernquist, L., & Kormendy, J. 2009, *ApJS*, 181, 486
- Jablonka, P., Martin, P., & Arimoto, N. 1996, *AJ*, 112, 1415
- Jablonka, P., Gorgas, J., & Goudfrooij, P. 2007, *A&A*, 474, 763
- Jaffe, Y. L., Aragon-Salamanca, A., De Lucia, G., Jablonka, P., Rudnick, G., Saglia, R., & Zaritsky, D. 2010, *arXiv:1007.1425*
- Janz, J., & Lisker, T. 2008, *ApJ*, 689, L25
- Jerjen, H., Binggeli, B., & Freeman, K. C. 2000, *AJ*, 119, 593
- Johnson, B. D., et al. 2007, *ApJS*, 173, 392
- Kannappan, S. J., Guie, J. M., & Baker, A. J. 2009, *AJ*, 138, 579
- Kawata, D., & Gibson, B. K. 2003, *MNRAS*, 340, 908
- Kelson, D. D., Illingworth, G. D., Franx, M., & van Dokkum, P. G. 2006, *ApJ*, 653, 159
- Kennicutt, R. C., Jr. 1989, *ApJ*, 344, 685
- Kim, K. O., & Ann, H. B. 1990, *Journal of Korean Astronomical Society*, 23, 43
- Kim, S., Rey, S.-C., Lisker, T., & Sohn, S. T. 2010, *ApJ*, 721, L72
- Klypin, A., Kravtsov, A. V., Valenzuela, O., & Prada, F. 1999, *ApJ*, 522, 82

- Kobayashi, C., & Arimoto, N. 1999, *ApJ*, 527, 573
- Kobayashi, C. 2004, *MNRAS*, 347, 740
- Koleva, M., Prugniel, P., De Rijcke, S., Zeilinger, W. W., & Michielsen, D. 2009, *Astronomische Nachrichten*, 330, 960
- Koo, D. C., et al. 2005, *ApJS*, 157, 175
- Kormendy, J., & Illingworth, G. 1983, *ApJ*, 265, 632
- Kormendy, J., & Kennicutt, R. C., Jr. 2004, *ARA&A*, 42, 603
- Kormendy, J., Fisher, D. B., Cornell, M. E., & Bender, R. 2009, *ApJS*, 182, 216
- Krajnović, D., et al. 2008, *MNRAS*, 390, 93
- Kronberger, T., Kapferer, W., Ferrari, C., Unterguggenberger, S., & Schindler, S. 2008, *A&A*, 481, 337
- La Barbera, F., de Carvalho, R. R., de la Rosa, I. G., Gal, R. R., Swindle, R., & Lopes, P. A. A. 2010, *arXiv:1006.4056*
- Larson, R. B. 1974, *MNRAS*, 166, 585
- Larson, R. B., Tinsley, B. M., & Caldwell, C. N. 1980, *ApJ*, 237, 692
- Lee, J. C., Kennicutt, R. C., Funes, S. J., José G., Sakai, S., & Akiyama, S. 2007, *ApJL*, 671, L113
- Lee, J. C., et al. 2009, *ApJ*, 706, 599
- Lin, D. N. C., & Faber, S. M. 1983, *ApJL*, 266, L21
- Lisker, T., Grebel, E. K., & Binggeli, B. 2006, *AJ*, 132, 497
- Lisker, T., Glatt, K., Westera, P., & Grebel, E. K. 2006, *AJ*, 132, 2432
- Lisker, T., Grebel, E. K., Binggeli, B., & Glatt, K. 2007, *ApJ*, 660, 1186
- Lisker, T., Grebel, E. K., & Binggeli, B. 2008, *AJ*, 135, 380
- Lisker, T., et al. 2009, *ApJL*, 706, L124
- MacArthur, L. A., Courteau, S., & Holtzman, J. A. 2003, *ApJ*, 582, 689
- MacArthur, L. A., Courteau, S., Bell, E., & Holtzman, J. A. 2004, *ApJS*, 152, 175



- MacArthur, L. A., Ellis, R. S., Treu, T., U, V., Bundy, K., & Moran, S. 2008, *ApJ*, 680, 70
- MacArthur, L. A., González, J. J., & Courteau, S. 2009, *MNRAS*, 395, 28
- MacArthur, L. A., McDonald, M., Courteau, S., & Gonzalez, J. J. 2010, *arXiv:1006.3831*
- Mac Low, M.-M., & Ferrara, A. 1999, *ApJ*, 513, 142
- Maraston, C. 2005, *MNRAS*, 362, 799
- Mayer, L., Governato, F., Colpi, M., Moore, B., Quinn, T., Wadsley, J., Stadel, J., & Lake, G. 2001, *ApJL*, 547, L123
- Mayer, L., Mastropietro, C., Wadsley, J., Stadel, J., & Moore, B. 2006, *MNRAS*, 369, 1021
- McDonald, M., Courteau, S., & Tully, R. B. 2009, *MNRAS*, 394, 2022
- McDonald, M., Courteau, S., Tully, R. B., & Roediger, J. 2011, *MNRAS*, 519 (Paper I)
- Mei, S., et al. 2007, *ApJ*, 655, 144
- Merritt, D. 2006, *Reports on Progress in Physics*, 69, 2513
- Michard, R. 2005, *A&A*, 441, 451
- Mihos, J. C., & Hernquist, L. 1996, *ApJ*, 464, 641
- Mihos, J. C. 2004, *Clusters of Galaxies: Probes of Cosmological Structure and Galaxy Evolution*, 277
- Mo, H. J., Mao, S., & White, S. D. M. 1998, *MNRAS*, 295, 319
- Moore, B., Katz, N., Lake, G., Dressler, A., & Oemler, A. 1996, *Nature*, 379, 613
- Moorthy, B. K., & Holtzman, J. A. 2006, *MNRAS*, 371, 583
- Muñoz-Mateos, J. C., Gil de Paz, A., Boissier, S., Zamorano, J., Jarrett, T., Gallego, J., & Madore, B. F. 2007, *ApJ*, 658, 1006
- Murphy, E. J., Kenney, J. D. P., Helou, G., Chung, A., & Howell, J. H. 2009, *ApJ*, 694, 1435
- Naab, T., Jesseit, R., & Burkert, A. 2006, *MNRAS*, 372, 839
- Neistein, E., van den Bosch, F. C., & Dekel, A. 2006, *MNRAS*, 372, 933

- Nelan, J. E., Smith, R. J., Hudson, M. J., Wegner, G. A., Lucey, J. R., Moore, S. A. W., Quinney, S. J., & Suntzeff, N. B. 2005, *ApJ*, 632, 137
- Noeske, K. G., et al. 2007, *ApJL*, 660, L43
- Ogando, R. L. C., Maia, M. A. G., Chiappini, C., Pellegrini, P. S., Schiavon, R. P., & da Costa, L. N. 2005, *ApJL*, 632, L61
- Paudel, S., Lisker, T., Kuntschner, H., Grebel, E. K., & Glatt, K. 2010, *MNRAS*, 405, 800
- Paudel, S., Lisker, T., & Kuntschner, H. 2011, *MNRAS*, 255
- Pedraz, S., Gorgas, J., Cardiel, N., Sánchez-Blázquez, P., & Guzmán, R. 2002, *MNRAS*, 332, L59
- Peletier, R. F., Balcells, M., Davies, R. L., Andredakis, Y., Vazdekis, A., Burkert, A., & Prada, F. 1999, *MNRAS*, 310, 703
- Pfenniger, D., & Norman, C. 1990, *ApJ*, 363, 391
- Pipino, A., D’Ercole, A., & Matteucci, F. 2008, *A&A*, 484, 679
- Pipino, A., D’Ercole, A., Chiappini, C., & Matteucci, F. 2010, *MNRAS*, 407, 1347
- Poggianti, B. M., Smail, I., Dressler, A., Couch, W. J., Barger, A. J., Butcher, H., Ellis, R. S., & Oemler, A., Jr. 1999, *ApJ*, 518, 576
- Rakos, K., & Schombert, J. 2004, *AJ*, 127, 1502
- Roediger, E., & Hensler, G. 2005, *A&A*, 433, 875
- Rogers, B., Ferreras, I., Peletier, R. F., & Silk, J. 2008, *arXiv:0812.2029*
- Roškar, R., Debattista, V. P., Stinson, G. S., Quinn, T. R., Kaufmann, T., & Wadsley, J. 2008, *ApJL*, 675, L65
- Saglia, R. P., Maraston, C., Greggio, L., Bender, R., & Ziegler, B. 2000, *A&A*, 360, 911
- Saglia, R. P., et al. 2010, *A&A*, 509, A61
- Sánchez-Blázquez, P., Gorgas, J., Cardiel, N., & González, J. J. 2006, *A&A*, 457, 809
- Sánchez-Blázquez, P., Forbes, D. A., Strader, J., Brodie, J., & Proctor, R. 2007, *MNRAS*, 377, 759
- Sanders, D. B., & Mirabel, I. F. 1996, *ARA&A*, 34, 749
- Serra, P., & Trager, S. C. 2007, *MNRAS*, 374, 769

- Skrutskie, M. F., et al. 2006, *AJ*, 131, 1163
- Smail, I., Ivison, R. J., & Blain, A. W. 1997, *ApJL*, 490, L5
- Smith, R. J., Lucey, J. R., & Hudson, M. J. 2007, *MNRAS*, 381, 1035
- Smith, R. J., Lucey, J. R., & Hudson, M. J. 2009, *MNRAS*, 400, 1690
- Sommer-Larsen, J., Götz, M., & Portinari, L. 2003, *ApJ*, 596, 47
- Somerville, R. S., & Primack, J. R. 1999, *MNRAS*, 310, 1087
- Spolaor, M., Proctor, R. N., Forbes, D. A., & Couch, W. J. 2009, *ApJL*, 691, L138
- Springel, V., et al. 2005, *Nature*, 435, 629
- Strader, J., Brodie, J. P., Spitler, L., & Beasley, M. A. 2006, *AJ*, 132, 2333
- Strateva, I., et al. 2001, *AJ*, 122, 1861
- Tamura, N., & Ohta, K. 2003, *AJ*, 126, 596
- Thomas, D., Greggio, L., & Bender, R. 1999, *MNRAS*, 302, 537
- Thomas, D., Maraston, C., Bender, R., & Mendes de Oliveira, C. 2005, *ApJ*, 621, 673
- Toloba, E., et al. 2009, *ApJL*, 707, L17
- Tolstoy, E., Hill, V., & Tosi, M. 2009, *ARA&A*, 47, 371
- Toomre, A., & Toomre, J. 1972, *ApJ*, 178, 623
- Tortora, C., Napolitano, N. R., Cardone, V. F., Capaccioli, M., Jetzer, P., & Molinaro, R. 2010, *MNRAS*, 407, 144
- Trager, S. C., Faber, S. M., Worthey, G., & González, J. J. 2000, *AJ*, 120, 165
- Trager, S. C., Faber, S. M., & Dressler, A. 2008, *MNRAS*, 386, 715
- Tremonti, C. A., et al. 2004, *ApJ*, 613, 898
- Valcke, S., de Rijcke, S., & Dejonghe, H. 2008, *MNRAS*, 389, 1111
- van der Wel, A., Holden, B. P., Zirm, A. W., Franx, M., Rettura, A., Illingworth, G. D., & Ford, H. C. 2008, *ApJ*, 688, 48
- van Dokkum, P. G. 2005, *AJ*, 130, 2647

- van Zee, L., Skillman, E. D., & Haynes, M. P. 2004, *AJ*, 128, 121
- van Zee, L., Barton, E. J., & Skillman, E. D. 2004, *AJ*, 128, 2797
- Vollmer, B., Cayatte, V., Balkowski, C., & Duschl, W. J. 2001, *ApJ*, 561, 708
- Weisz, D. R., Skillman, E. D., Cannon, J. M., Dolphin, A. E., Kennicutt, R. C., Jr., Lee, J., & Walter, F. 2008, *ApJ*, 689, 160
- White, S. D. M. 1980, *MNRAS*, 191, 1P
- Witt, A. N., Thronson, H. A., Jr., & Capuano, J. M., Jr. 1992, *ApJ*, 393, 611
- Wu, H., Shao, Z., Mo, H. J., Xia, X., & Deng, Z. 2005, *ApJ*, 622, 244
- Xilouris, E. M., Byun, Y. I., Kylafis, N. D., Paleologou, E. V., & Papamastorakis, J. 1999, *A&A*, 344, 868
- Zaritsky, D., Kennicutt, R. C., Jr., & Huchra, J. P. 1994, *ApJ*, 420, 87

Table 1. Explored star formation histories for stellar population modeling

SFH	$\Psi(t)$ ( $M_{\odot} \text{ Gyr}^{-1}$ )	$\langle A \rangle (\tau, A)$ (Gyr)	$\tau$ range (Gyr)	$\langle A \rangle$ range (Gyr)
(1)	(2)	(3)	(4)	(5)
Constant	constant = $\frac{1}{\tau}$	$A - \frac{\tau}{2}$	[0.2, 13]	6.5 - 12.9
Delayed	$\frac{t}{\tau^2} e^{(-t/\tau)}$	$A - 2 \frac{\tau - e^{-A/\tau} \left( \tau + A + \frac{A^2}{2\tau} \right)}{1 + \frac{A}{\tau} (1 - e^{-A/\tau})}$	$[-\infty, \infty]$	0.9 - 12.9
Exponential	$\frac{1}{\tau} e^{-t/\tau}$	$A - \tau \frac{1 - e^{-A/\tau} \left( 1 + \frac{A}{\tau} \right)}{1 - e^{-A/\tau}}$	$[-\infty, \infty]$	0.9 - 12.9
Linear	$\frac{2}{\tau} \left[ 1 - \left( \frac{t}{\tau} \right) \right]$ , for $t < \tau$ 0, for $t \geq \tau$	$A - \frac{\tau}{3}$	[0.3, 36.3]	0.9 - 12.9
Sandage	$\frac{t}{\tau^2} e^{(-t^2/2\tau^2)}$	$A - \frac{(1/2)\tau\sqrt{2\pi} \operatorname{erf}(A/\sqrt{2}\tau) - Ae^{-A^2/2\tau^2}}{1 - e^{-A^2/2\tau^2}}$	[0.08, $\infty$ ]	4.4 - 12.9
Single-burst	$\delta(t)$	$A - t$	[0.0, 12.1]	0.9 - 13.0

Table 2. Median age gradients of Virgo galaxies

Morphology	$\frac{d\langle A \rangle}{dr}$			$\langle A \rangle_0$	$N$
	$r/r_e$ ( $\text{Gyr } r_e^{-1}$ )	$r$ ( $\text{Gyr kpc}^{-1}$ )	$\log r$ ( $\text{Gyr dex}^{-1}$ )	(Gyr)	
(1)	(2)	(3)	(4)	(5)	(6)
dS0	$0.05 \pm 1.13$	$0.03 \pm 0.89$	$0.12 \pm 1.90$	$9.65 \pm 0.99$	19
dE	$0.22 \pm 1.45$	$0.30 \pm 1.26$	$0.34 \pm 2.50$	$9.68 \pm 1.14$	49
E	$0.30 \pm 0.91$	$0.27 \pm 1.96$	$0.84 \pm 3.05$	$10.15 \pm 0.82$	31
S0	$0.00 \pm 0.62$	$0.00 \pm 0.58$	$-0.07 \pm 1.50$	$10.20 \pm 0.70$	53
Sa–Sb	$0.02 \pm 0.73$	$0.01 \pm 0.55$	$0.02 \pm 1.59$	$10.00 \pm 1.27$	24
Sbc+Sc	$0.26 \pm 1.49$	$0.13 \pm 0.60$	$0.41 \pm 2.25$	$9.20 \pm 1.44$	15
Scd+Sd	$-0.13 \pm 1.19$	$-0.10 \pm 0.84$	$-0.53 \pm 2.40$	$8.95 \pm 1.70$	17
Sdm+Sm	$0.58 \pm 1.98$	$0.28 \pm 0.93$	$0.71 \pm 2.38$	$7.20 \pm 2.37$	9
Im	$1.31 \pm 3.08$	$1.03 \pm 2.86$	$2.05 \pm 4.55$	$5.15 \pm 2.98$	13
BCD	$2.07 \pm 2.68$	$1.92 \pm 4.85$	$4.25 \pm 5.64$	$5.60 \pm 2.08$	8
S?	$1.16 \pm 1.55$	$1.01 \pm 1.03$	$2.80 \pm 2.60$	$6.50 \pm 3.19$	9
?	$0.58 \pm 0.99$	$0.18 \pm 2.15$	$1.26 \pm 2.44$	$9.15 \pm 1.68$	8

Table 3. Median metallicity gradients of Virgo galaxies

Morphology	$\frac{d\log(Z/Z_{\odot})}{dr}$		$\log(Z_0/Z_{\odot})$		$N$
	$r/r_e$ (dex $r_e^{-1}$ )	$r$ (dex kpc $^{-1}$ )	$\log r$	(dex)	
(1)	(2)	(3)	(4)	(5)	(6)
dS0	$-0.10 \pm 0.30$	$-0.05 \pm 0.27$	$-0.16 \pm 0.54$	$-0.21 \pm 0.29$	19
dE	$-0.23 \pm 0.43$	$-0.18 \pm 0.43$	$-0.46 \pm 0.84$	$-0.49 \pm 0.22$	49
E	$-0.17 \pm 0.25$	$-0.14 \pm 0.60$	$-0.60 \pm 0.89$	$+0.05 \pm 0.36$	31
S0	$-0.06 \pm 0.24$	$-0.04 \pm 0.21$	$-0.27 \pm 0.47$	$+0.01 \pm 0.25$	53
Sa–Sb	$-0.13 \pm 0.26$	$-0.05 \pm 0.10$	$-0.34 \pm 0.53$	$-0.07 \pm 0.27$	24
Sbc+Sc	$-0.25 \pm 0.43$	$-0.09 \pm 0.18$	$-0.48 \pm 0.62$	$-0.08 \pm 0.32$	15
Scd+Sd	$-0.25 \pm 0.70$	$-0.11 \pm 0.57$	$-0.38 \pm 2.03$	$-0.09 \pm 0.65$	17
Sdm+Sm	$-0.15 \pm 0.93$	$-0.08 \pm 0.69$	$-0.28 \pm 1.44$	$-0.25 \pm 0.34$	9
Im	$-0.68 \pm 1.02$	$-0.30 \pm 1.06$	$-0.86 \pm 1.78$	$-0.40 \pm 0.41$	13
BCD	$-0.32 \pm 0.36$	$-0.36 \pm 0.56$	$-0.63 \pm 0.67$	$-0.40 \pm 0.19$	8
S?	$-0.31 \pm 0.55$	$-0.26 \pm 0.34$	$-0.42 \pm 0.74$	$-0.47 \pm 0.38$	9
?	$-0.20 \pm 0.45$	$-0.08 \pm 0.97$	$-0.54 \pm 1.13$	$+0.01 \pm 0.57$	8

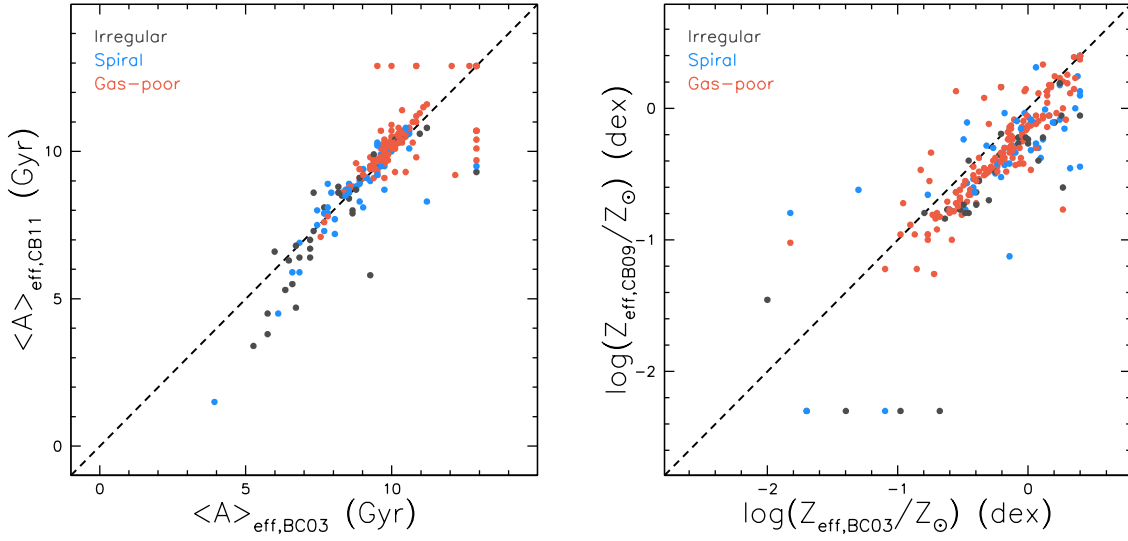


Fig. 1.— (*left*) Comparison of the mean ages measured at the effective radii,  $r_e$ , of all Virgo galaxies based on either the Bruzual & Charlot (2003) or Charlot & Bruzual (2010) models. The data points have been coloured according to basic galaxy type (gas-poor, spiral, irregular). The dashed line shows the locus of equality. (*right*) Same as (*left*) but for metallicities.

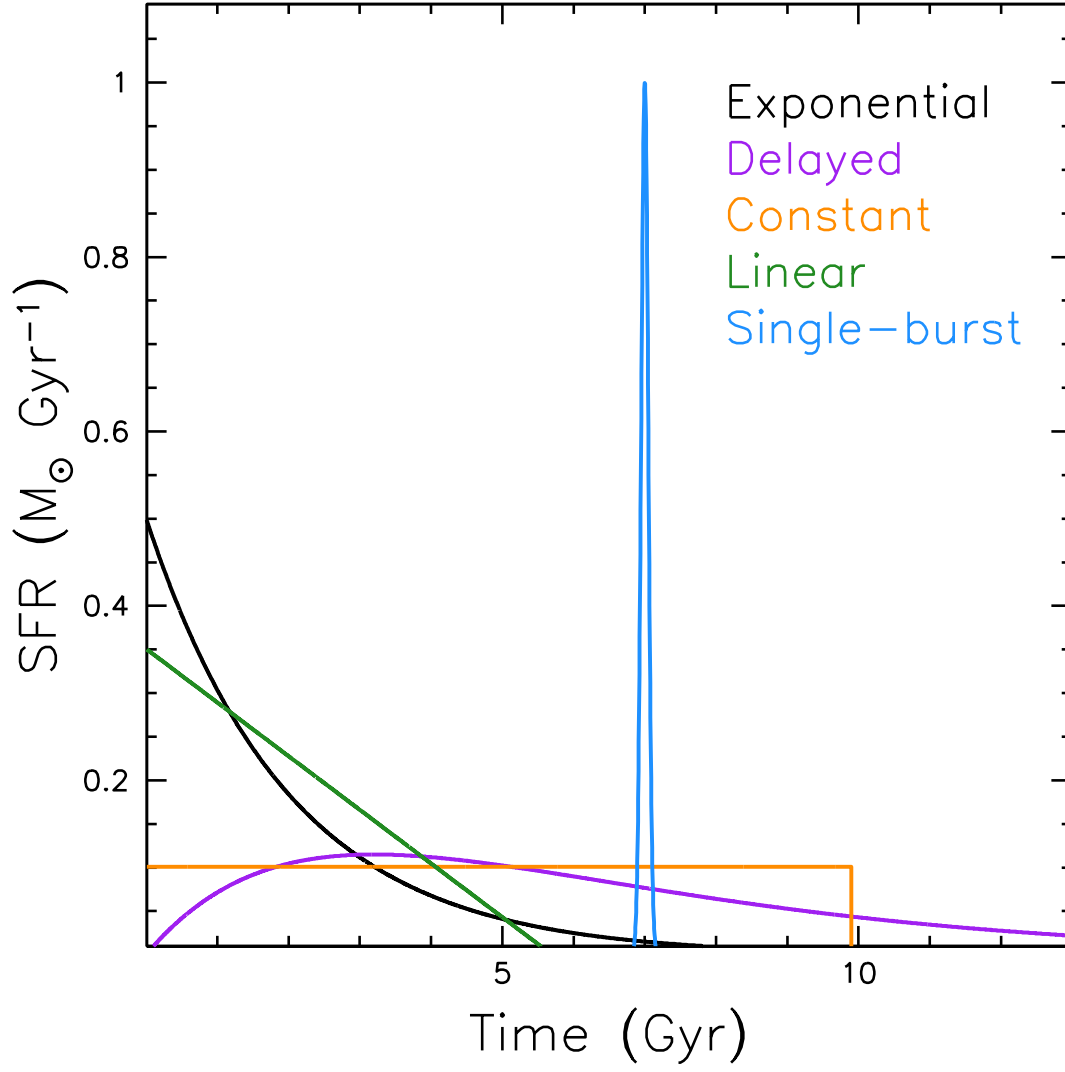


Fig. 2.— Representative star formation histories (SFHs) explored in our stellar population modeling. Each curve is normalized to produce a stellar mass of unity at 13 Gyr.



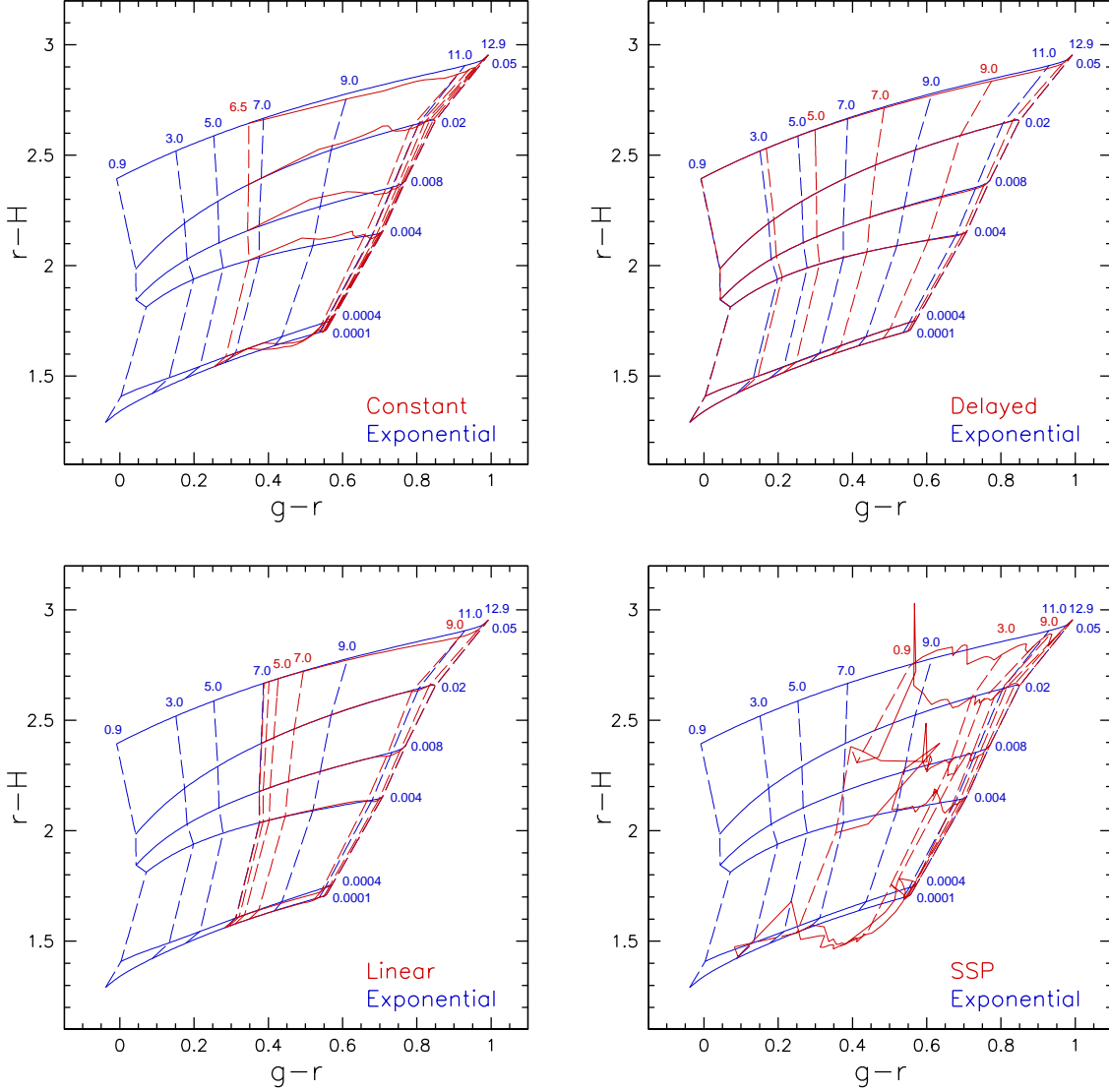


Fig. 3.— Predictions of the  $r-H$  versus  $g-r$  colour grids from Charlot & Bruzual (2010) stellar population models for a (*upper left*) constant, (*upper right*) delayed, (*lower left*) linear, and (*lower right*) single-burst SFH. The dashed and solid lines represent loci of constant mean age and metallicity, respectively. The predictions of an exponential SFH model are shown in each panel for comparison.

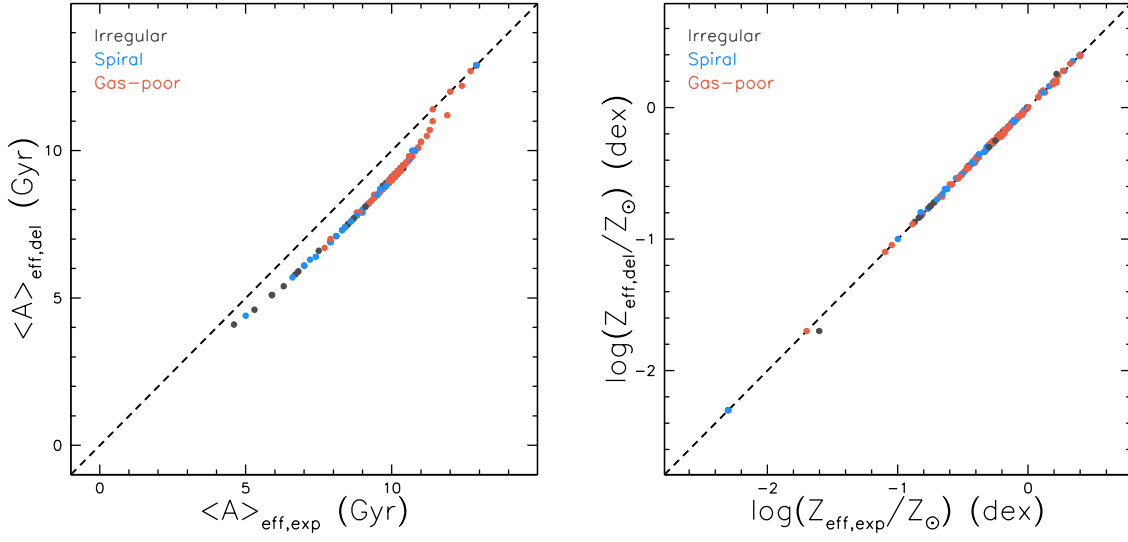


Fig. 4.— (*left*) Comparison of the mean ages measured at  $r_e$  for all Virgo galaxies based on either a delayed or exponential SFH. The data points have been coloured according to basic galaxy type (gas-poor, spiral, irregular). The dashed line shows the locus of equality. (*right*) Same as (*left*) but for metallicities.

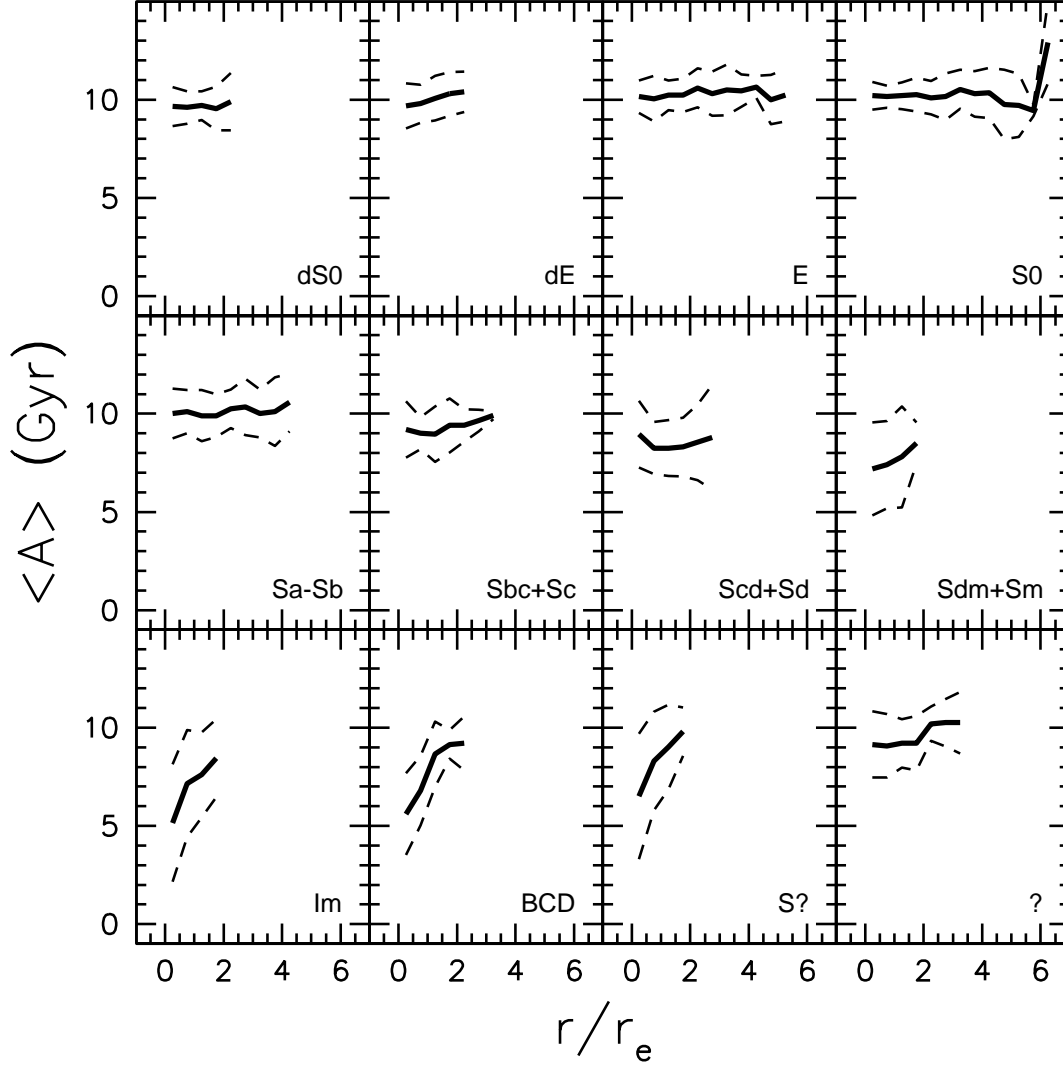


Fig. 5.— Mean age profiles as a function of scaled radius for Virgo galaxies, binned by morphology. The median profiles and their rms dispersions are indicated by the thick solid and dashed lines, respectively.

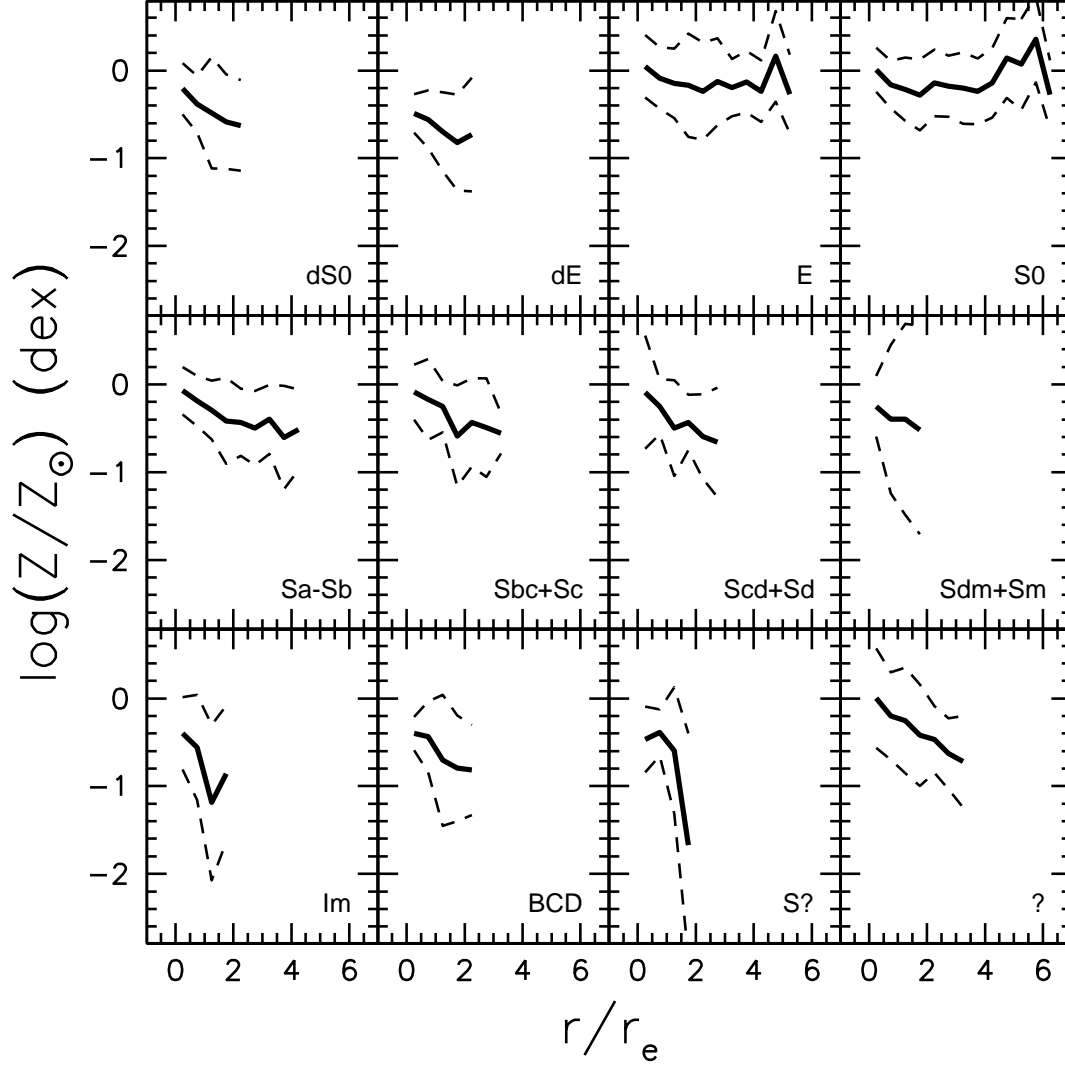


Fig. 6.— As in Figure 5 but for metallicity profiles.

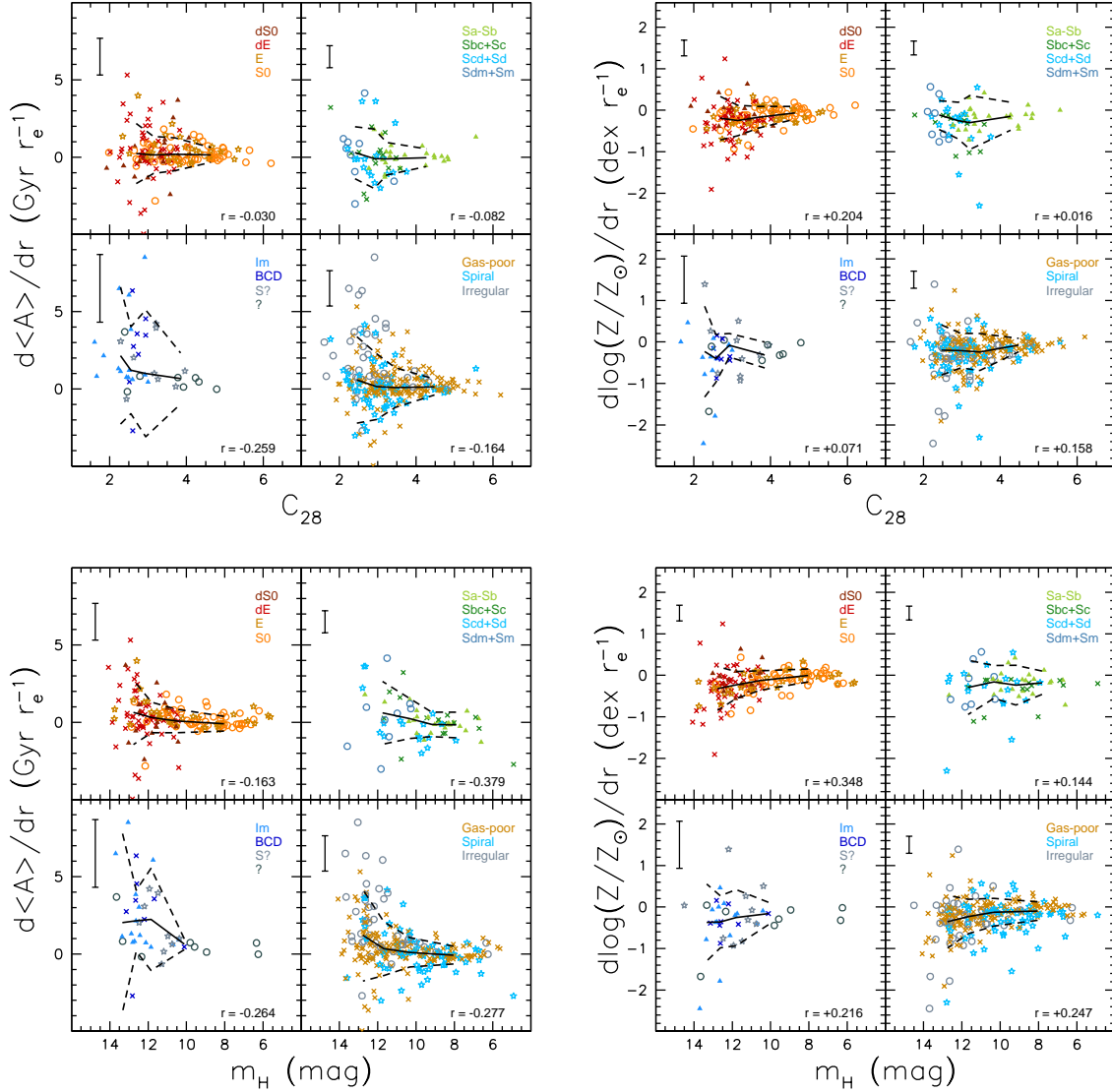


Fig. 7.— Mean age gradients (*top-left*) and metallicity gradients (*top-right*) versus  $H$ -band concentrations for Virgo galaxies, binned by basic galaxy type (gas-poor, spiral and irregular). The gradients are expressed in terms of the scaled radius  $r/r_e$ , while individual galaxies are separated by specific morphology. The median trend (solid line) and its rms dispersion (dashed lines), the Pearson correlation coefficient, and the typical error per point are shown in each window. The bottom two plots are as at top, but shown versus apparent  $H$ -band magnitudes.

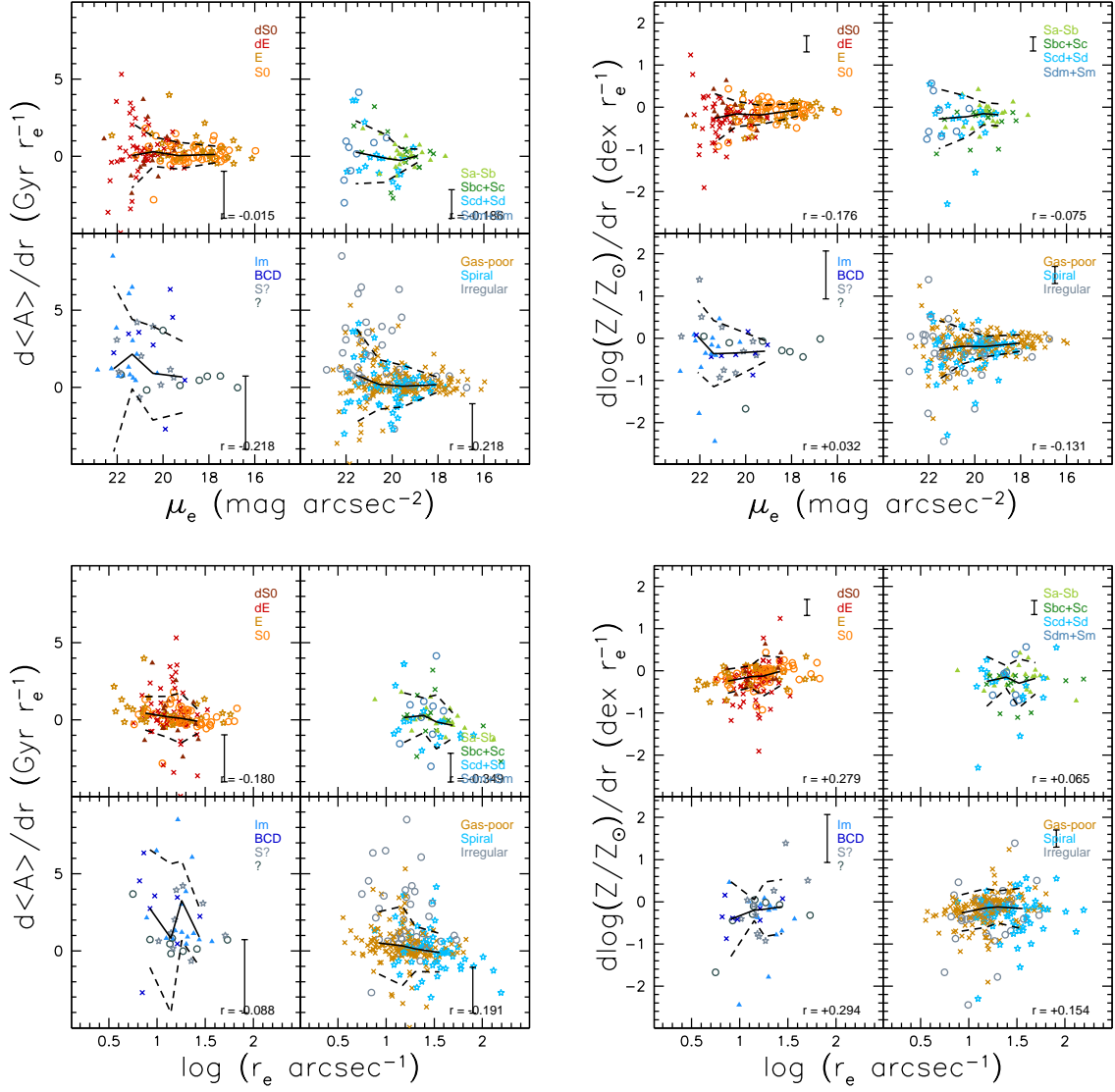


Fig. 8.— As in Figure 7 but versus  $H$ -band effective surface brightnesses (*top*) and effective radii (*bottom*).

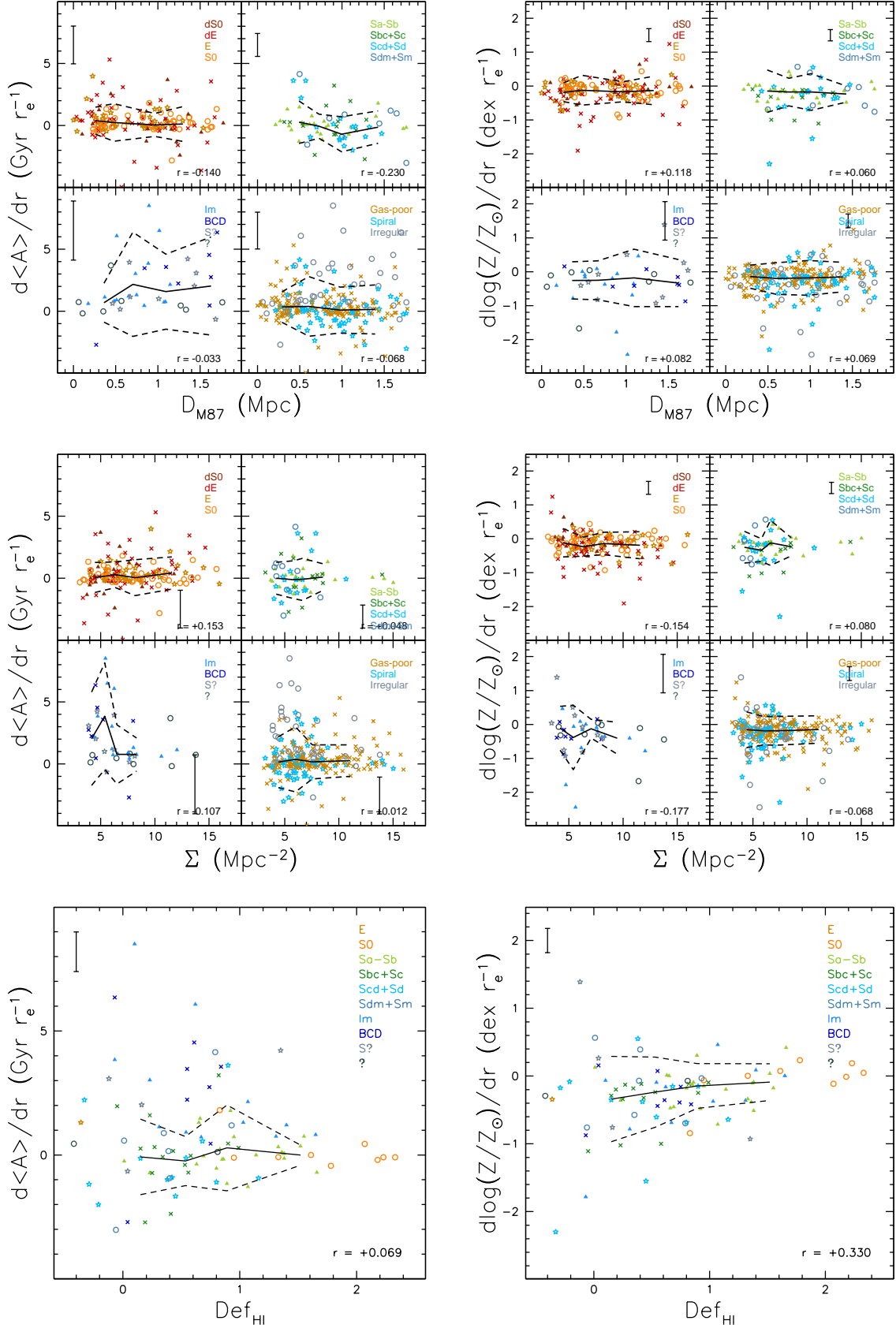


Fig. 9.— As in Figure 7 but versus cluster-centric distances (*top*), galaxy surface densities (*middle*), and HI gas deficiencies (*bottom*).

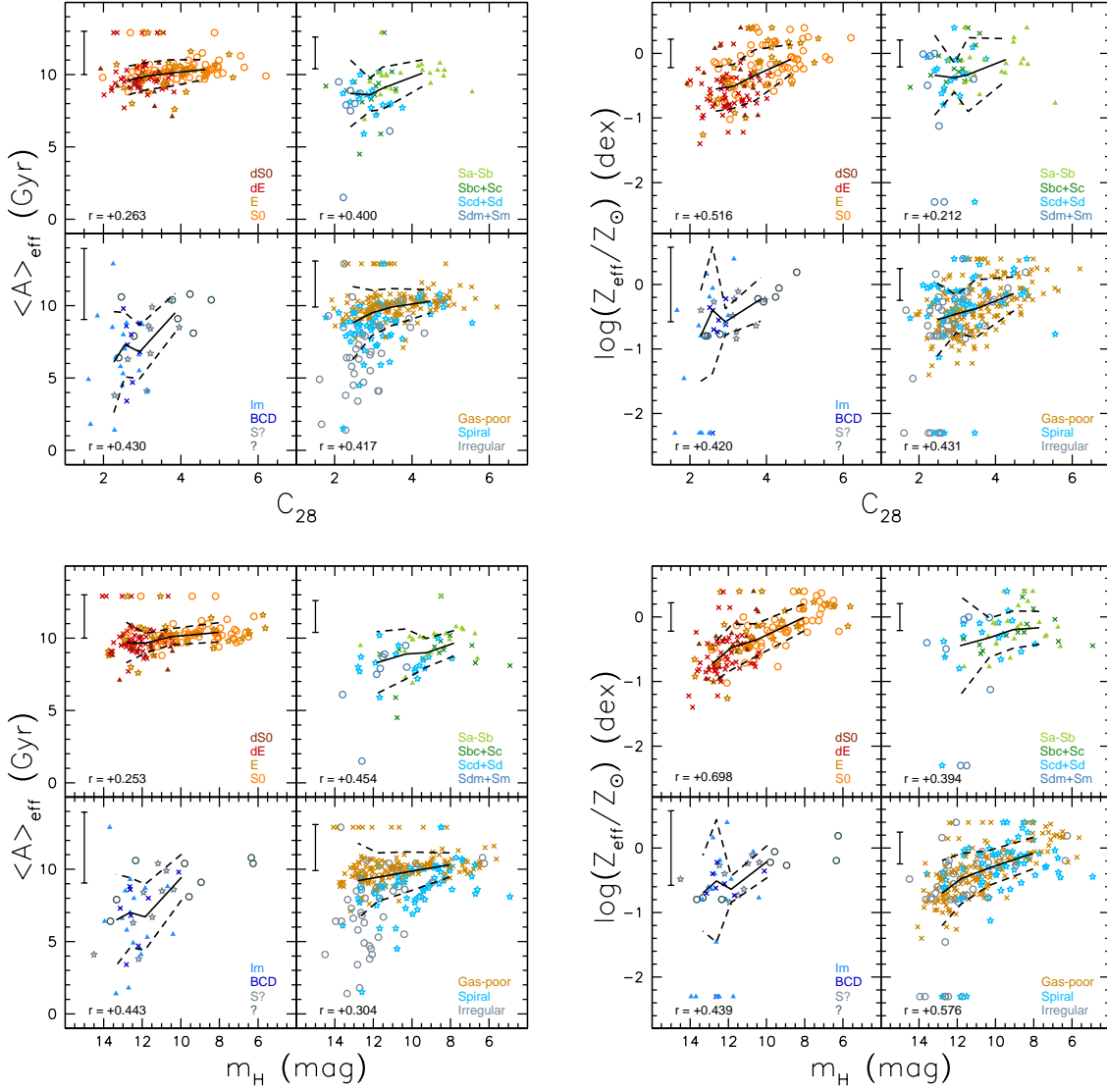


Fig. 10.— As in Figure 7 but for the (*left*) mean ages and (*right*) metallicities of Virgo galaxies measured at  $r_e$ .



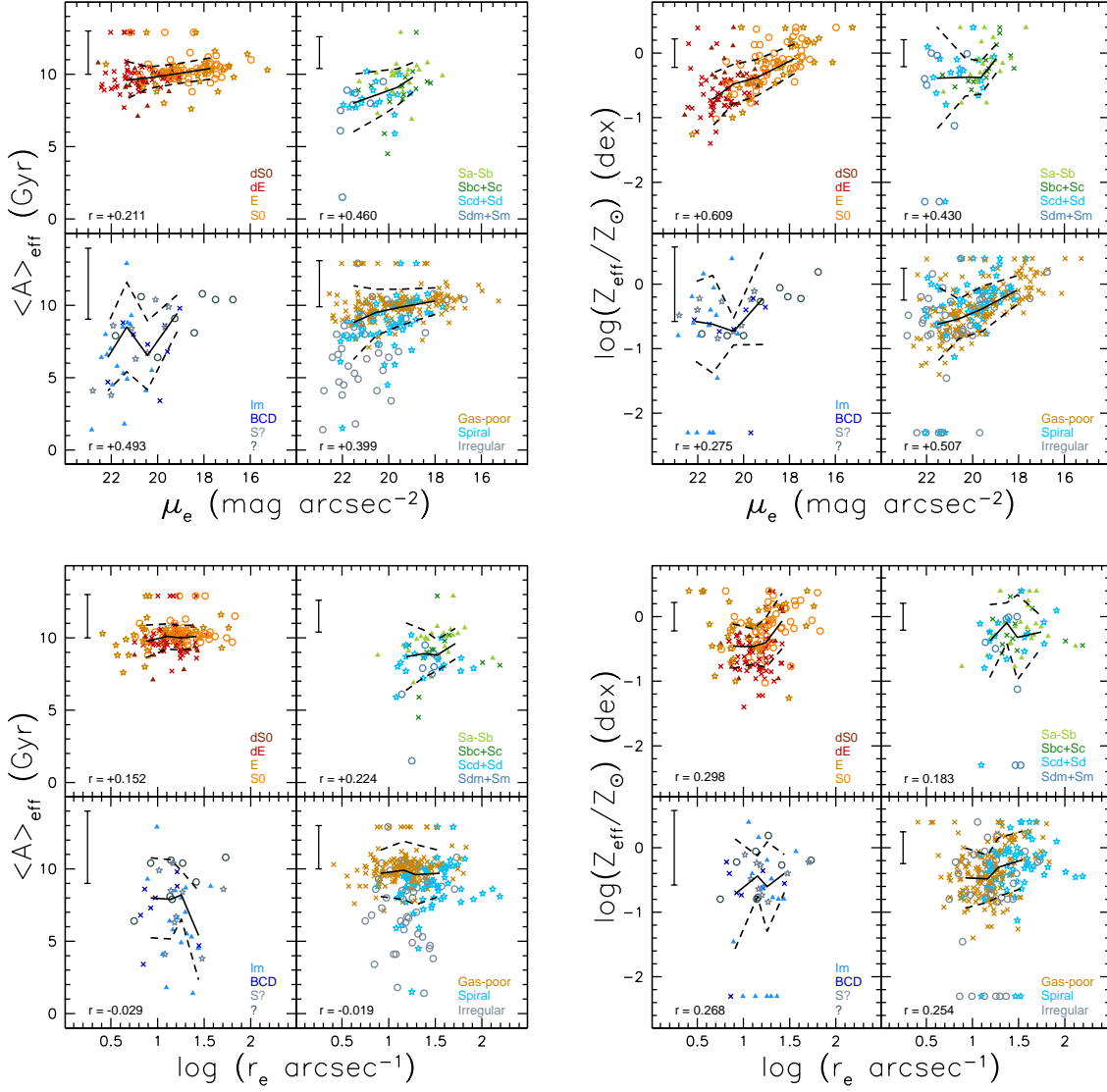


Fig. 11.— As in Figure 10 but versus  $H$ -band effective surface brightnesses (*top*) and effective radii (*bottom*).

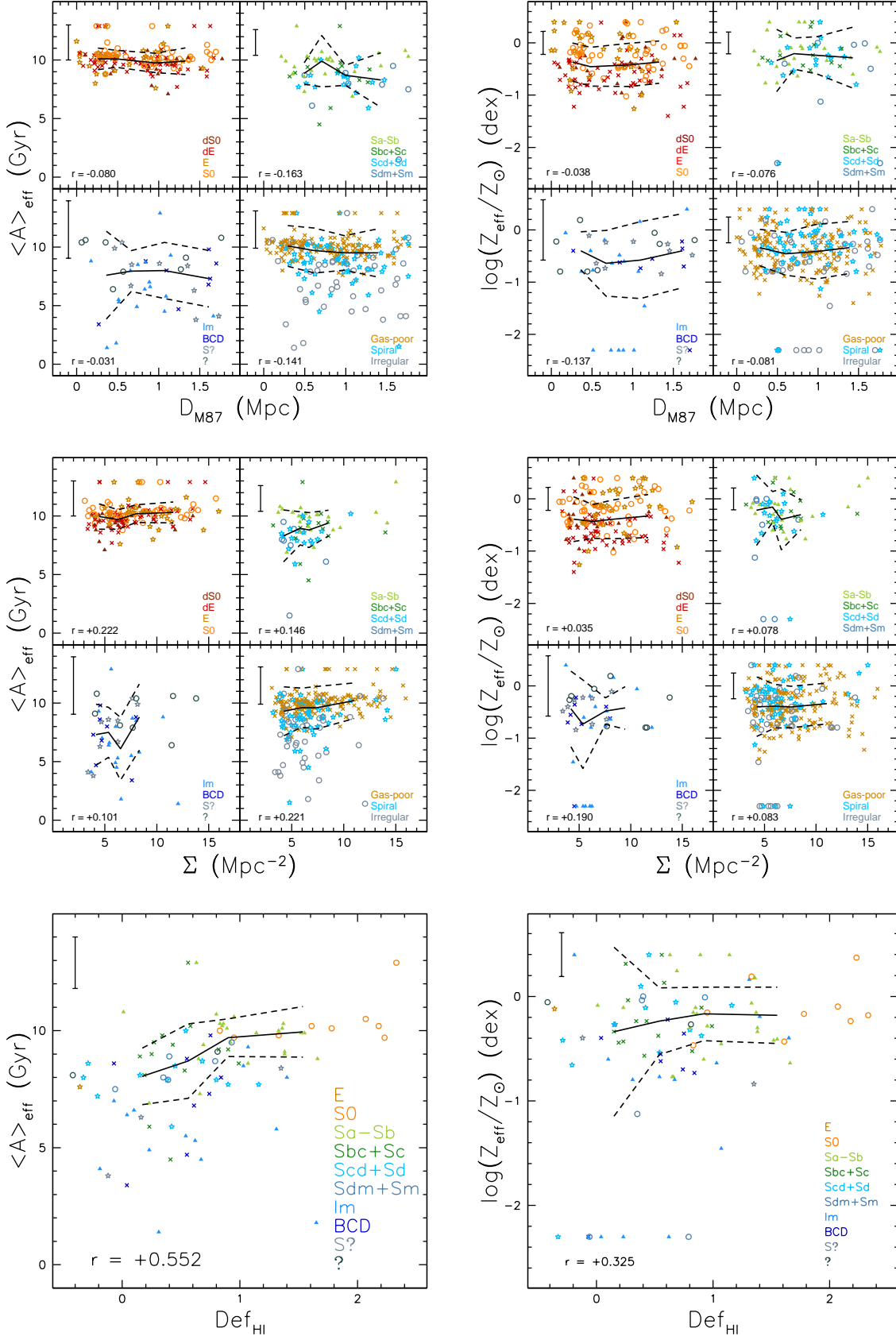


Fig. 12.— As in Figure 7 but versus cluster-centric distances (*top*), galaxy surface densities (*middle*), and HI gas deficiencies (*bottom*).

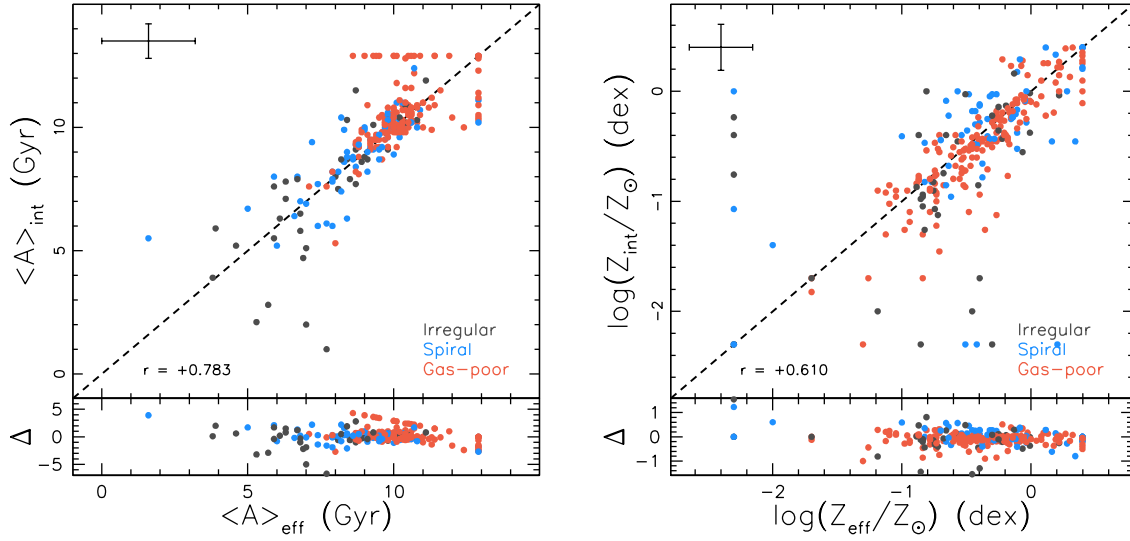


Fig. 13.— (*left*) Integrated mean ages versus mean ages measured at  $r_e$  for all Virgo galaxies. The data points for individual galaxies have been coloured according to their specific morphology. Direct equality (solid line), the Pearson correlation coefficient, and the typical error per point are also shown in each plot. (*right*) Same as (*left*) but for metallicities.

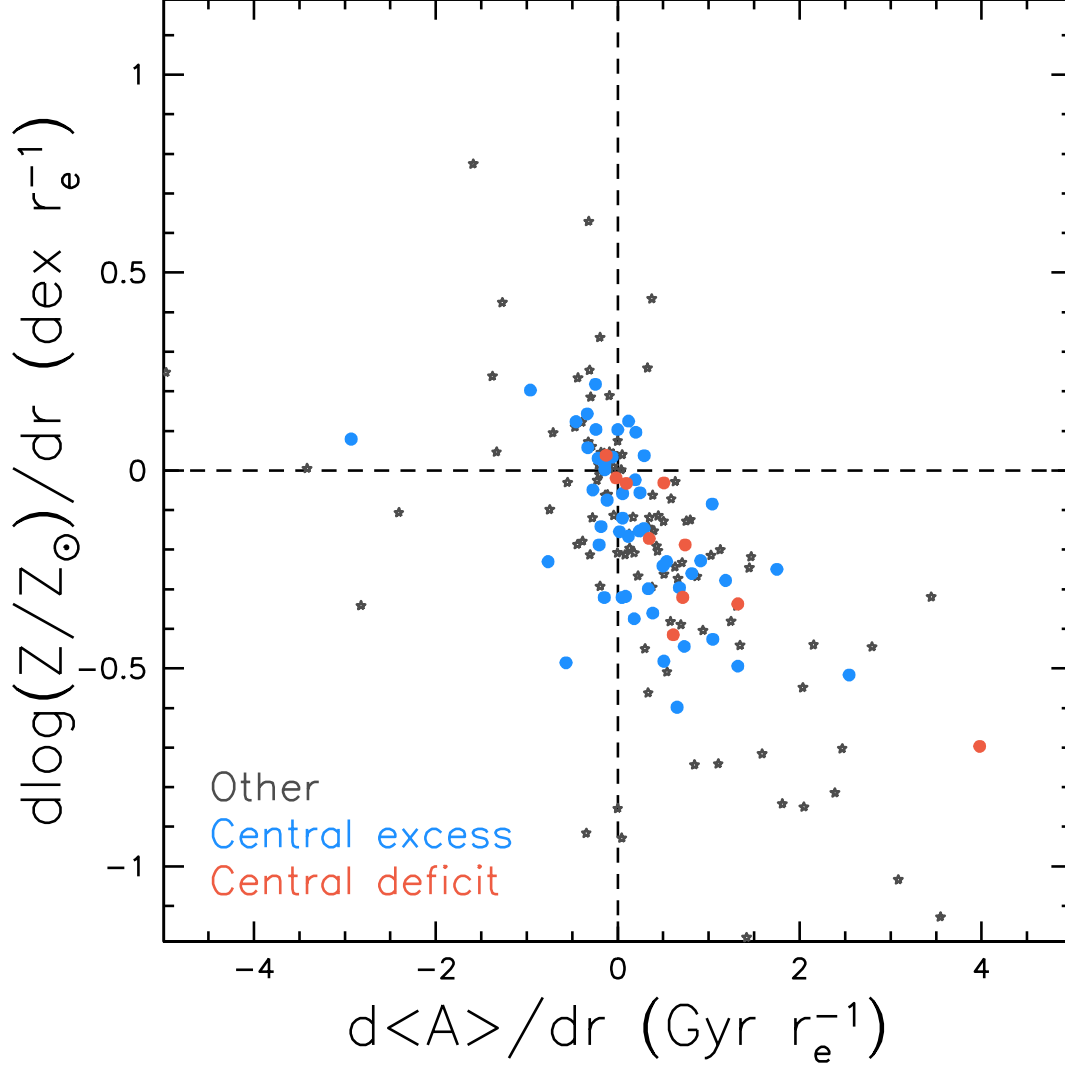


Fig. 14.— Metallicity gradients versus age gradients for Virgo gas-poor galaxies. The circular points represent those galaxies whose central light profiles have been analysed by Côté et al. (2006); the colours of these data points denote a central light excess or deficit. The Virgo gas-poor galaxies whose central light behaviour has not yet been analysed are represented by dark grey stars.

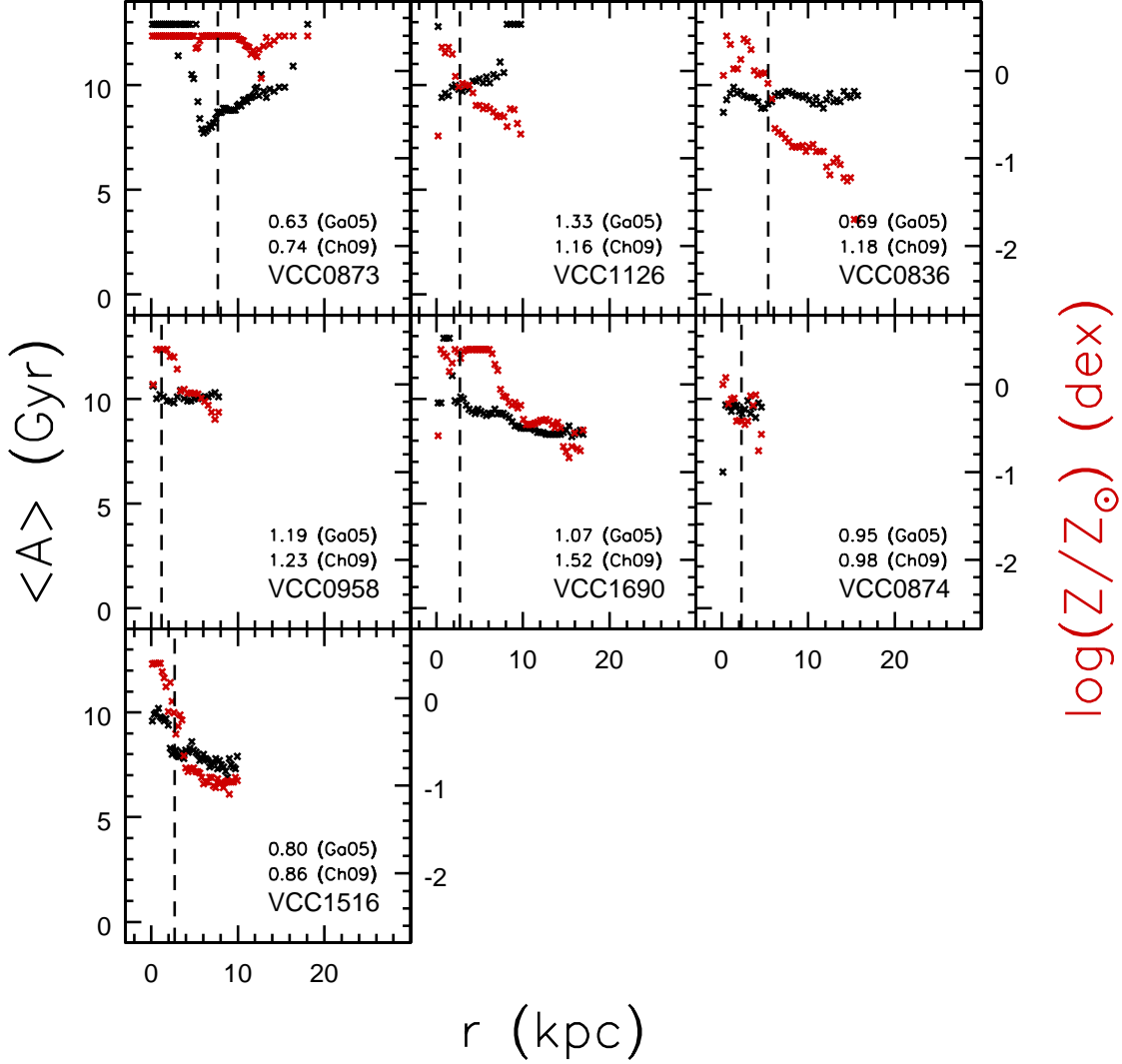


Fig. 15.— Age (black) and metallicity (red) profiles for Virgo spiral galaxies which overlap with the Crowl & Kenney (2008) sample. For each galaxy, we provide in the bottom right corner of each window the Virgo Cluster Catalog identification number and the  $Def_{HI}$  values from both Gavazzi et al. (2005) and Chung et al. (2009, Ch09).

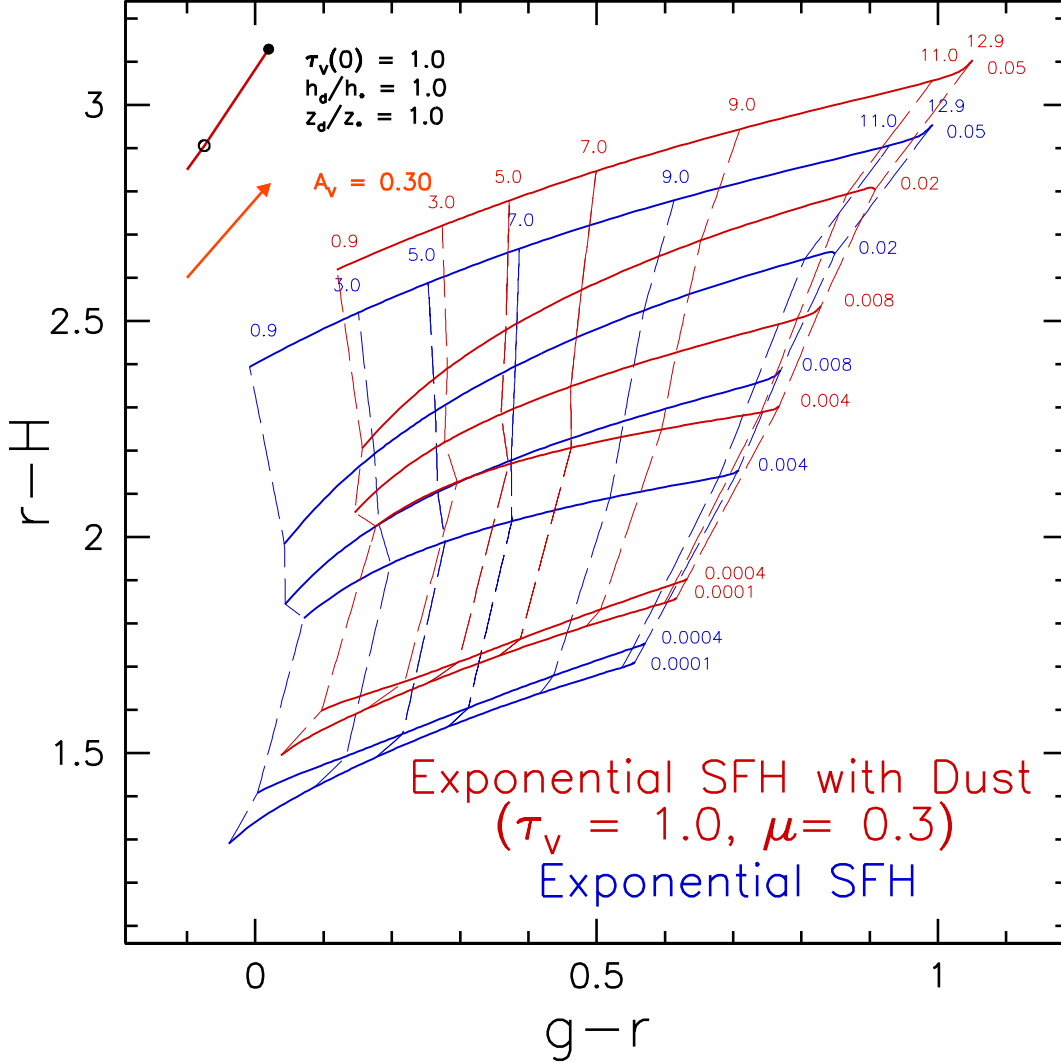


Fig. 16.— As in Figure 3 but comparing an exponential SFH model with (red) and without (blue) reddening, whereby a clumpy medium dust model was used for the former. The reddening vectors for the foreground screen and face-on triplex models (orange-red and dark-red, respectively) are also shown. Parameter values for the clumpy model are indicated at lower-right in each panel ( $\tau_V$  = V-band optical depth of molecular cloud;  $\mu$  = relative optical depth of diffuse ISM), while those for the other models are adjacent to the vectors themselves. The position of the galaxy's center and half-light radius in the triplex vector are indicated by the solid and open circles, respectively.